5
PERFORMANCE OF SIZED YARNS

5.1 INTRODUCTION

The ideal and most reliable evaluation of sized yarn performance can be made during the actual weaving operation. The process of evaluating sized yarns, sizing ingredients, and various size formulations by an actual weaving trial, albeit not impossible, is time consuming, risky, and prohibitively expensive. In research, where a quick and reliable estimation is required, some other means of assessment and criteria ultimately linked to weaveability will have to be developed. The criteria used should yield maximal and reliable information, yet should be sufficiently quick to assess [1]. To assess the efficiency of a variety of size formulations and the effect of slashing variables under a wide range of weaving conditions, it is imperative that a laboratory evaluation system is established [2–7]. This chapter discusses the importance of the laboratory evaluation of sized yarns and its correlation to weaveability.

The factors that affect the weaveability of warp yarns are diverse and numerous. Table 5.1 shows the dependence of weaveability on sized warps [8]. The consideration of the sizing process, in terms of processing the warp on the loom at maximal efficiency, is a ''macro aspect.'' On the other hand, the consideration and control of thousands of warp yarns on the beam precisely during the process of weaving involves a ''micro aspect'' of sizing [8]. Even one yarn going out of its place or one broken end causes stoppage of the weaving process, and the mending of such a broken warp end results in imperfection in the cloth. The micro aspect of the sizing process requires an under-

standing of the stresses and the abrasive action that the warp yarns have to withstand during weaving, the nature of imperfections, such as thick and thin places in an unsized yarn, and the characteristics of sizing ingredients and the size add-on level that protects the weak places in a yarn.

5.2 CRITERIA OF ASSESSMENT

Various criteria have been used in characterizing warp yarn performance, which include the objective assessment of yarn properties before and after slashing. The criteria used may be broadly categorized in the following groups:

1. Tensile strength and elongation
2. Cohesiveness and adhesion of size film
3. Abrasion resistance of sized yarns
4. Fatigue and abrasion of sized yarns (under cyclic loading in tension, bending, and shear)

5.2.1 Tensile Strength and Elongation

Earlier attempts to assess weaveability were directed toward the assessment of the tensile strength and elongation at break of yarns before and after sizing. The increase in tensile strength was taken as a criterion to correlate with weaveability [9–11]. As expected, this approach has not shown consistent correlation with actual weaving performance since the actual tension experienced by a yarn during weaving rarely exceeds 20% of the breaking strength of a yarn [8,10,11]. Even unsized yarns in many instances have at least this minimum requirement of strength and elongation at break. Another approach used to assess the performance of sizing materials has been to apply sizing ingredients, such as starches, to desized cloth and then test the strength, elongation, stiffness, smoothness, and crushability of the resulting fabrics [12–14].

5.2.2 Cohesiveness and Adhesion of Sized Films

In this criterion the physical and mechanical properties of size films have been studied [15–18]. To determine the cohesiveness of the size film, a thin film of size is cast and evaluated for strength, elongation at break, stiffness, and tackiness properties. The results are usually normalized by using the weight or thickness of the specimen to facilitate comparison between size films made from different ingredients and size formulations. Faasen and van Harten [10] prepared size films by pouring sizing solutions on a flat methacrylate plate.

Table 5.1 Dependence of Weaveability on Sized Warp

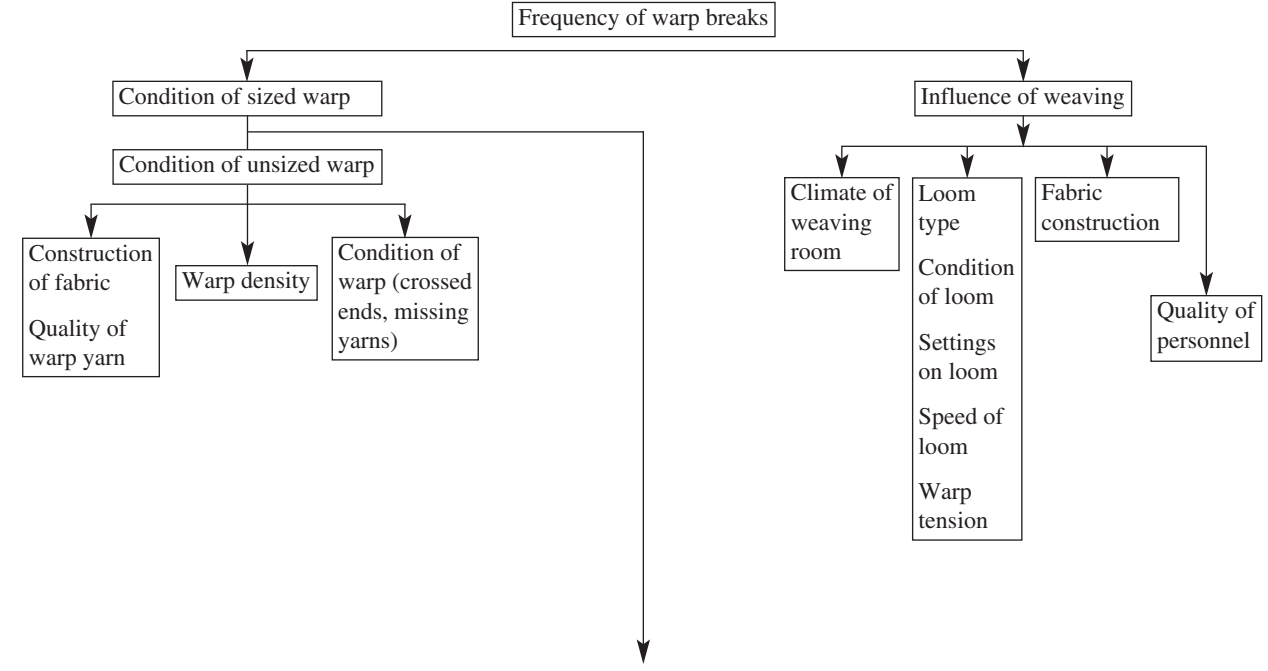

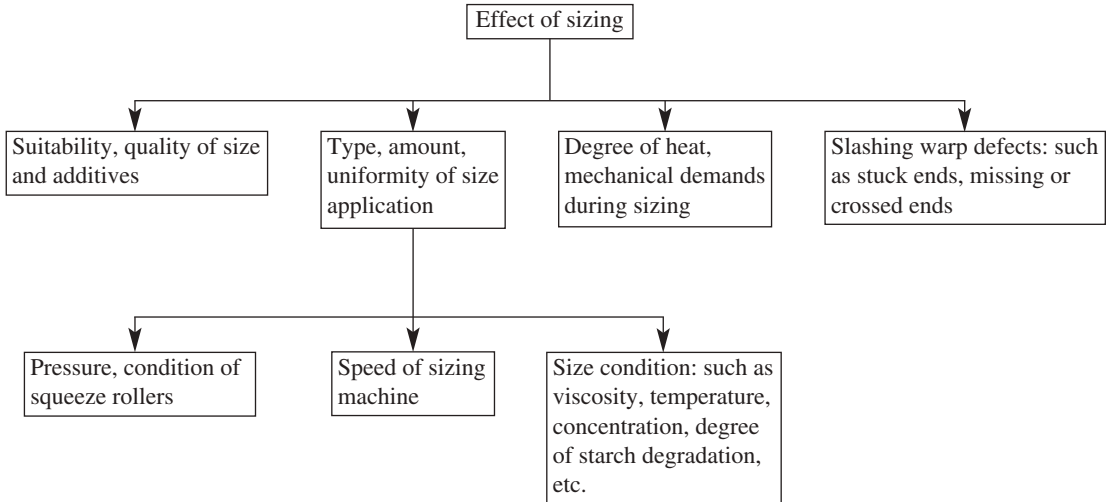

Source: Ref. 8.

The methacrylate plate used was found to be the most suitable as the films could be easily peeled off. The films were carefully dried in an oven at approximately 40°C. The 10-mm-wide film strips were then conditioned at 20°C and at various relative humidities for several days. The tensile testing of the size films at a gauge length of 100 mm was carried out on an electronic dynamometer operating on the principle of constant rate of extension. Table 5.2 shows the results of the experiments on various size films performed at different relative humidities [10]. In general, on increasing the relative humidity from 45 to 65%, the strength of the starch products increased, whereas those of sodium alginate and sodium carboxymethyl cellulose (SCMC) decreased. However, increasing the relative humidity from 65 to 85% reduced the strength of all size films. The extension of films made from sodium alginate and starch ether increases significantly with an increase in relative humidity from 65 to 85%, as shown in Table 5.2. Films of SCMC (B) and starch ether become sticky at a relative humidity of 85% and show a tendency to flow. Such products are, therefore, unsuitable for use in a weaving room where relative humidities are generally in the vicinity of 85%. Potato starch, oxidized potato starch, and a mixture of potato starch and sodium alginate are reasonably stable toward changes in relative humidity. However, it is hard to visualize that the studies on size films alone will yield adequate correlation with weavability since the measurements are made exclusively on size without the ''reinforcing'' action of the yarns or fibers [19].

Compatibility of the size with the textile materials, in other words the ''adhesive power'' of the size to substrate, has been evaluated by sizing a roving and then determining its tensile strength [19–21]. The adhesive power is then defined as a ratio of the tensile strength at a gauge length l to the tensile strength at zero gauge length:

$$\text{adhesive power} = \frac{\text{tensile strength of sized roving at gauge length, } l}{\text{tensile strength of sized roving at zero gauge length}}$$

A typical relationship between adhesive power versus size add-on is shown in Fig. 5.1; a ''good'' sized roving can be distinguished from the roving that is ''badly'' sized. The adhesive power of the well-sized roving increases linearly with an increase in add-on of up to about 5%, beyond which the slashed roving yields. Such studies provide useful guidelines regarding the relative adhesive characteristics of different size ingredients with different types of fibers. Figure 5.2 shows a typical stress–strain diagram of a sized roving at a gauge length l. King et al. [19] have used the criterion of roving strength in establishing the differences between sizing formulations, as shown in Figs.

Table 5.2 Mechanical Properties of Size Films

Sizing ingredient	45% RH		65% RH		85% RH	
	Strength (kg/mm^2)	Breaking extension (%)	Strength (kg/mm^2)	Breaking extension (%)	Strength (kg/mm^2)	Breaking extension (%)
Potato starch	2.4	3.3	3.5	2.0	2.6	2.3
Oxidized potato starch	3.2	4.2	4.1	2.0	3.5	2.5
Starch ether	1.2	3.8	2.1	1.8	0.4	29.9
Sodium alginate	2.7	7.7	2.3	5.9	2.5	16.5
Potato starch + sodium alginate (3 : 1)	3.6	5.9	3.3	3.7	2.8	3.6
SCMC (A)	9.8	11.5	6.0	15.0	3.7	17.2
SCMC (B)	3.9	31.5	3.3	32.0	1.6	86.0

Note: SCMC: sodium carboxymethyl cellulose.
Source: Ref. 10.

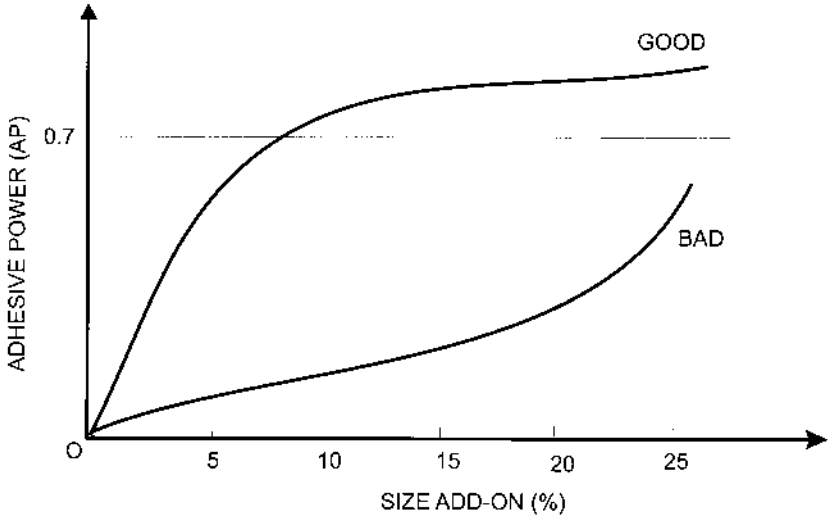

Fig. 5.1 Adhesive power of size versus size add-on. (From Ref. 21.)

5.3 to 5.8. They used six different hanks of roving. The broken lines in all these figures indicate the respective property of the unsized roving. The solid lines indicate the strength of the respective rovings at various size formulations. For example, in Fig. 5.3, the application of a 2% solution of starch (Clinco 15) resulted in an increase in strength of the roving from 90 gf to 570 gf (curve E); the addition of a similar quantity of Methocel (100 cps) gave a strength of 1440 gf (Fig. 5.4, curve Q). On the other hand, the differences in ultimate elongations of the rovings treated with the above sizing agents are small, as shown in Figs. 5.5 and 5.6. Similarly, the bending lengths are about the same, as shown in Figs. 5.7 and 5.8. Figure 5.9 shows the relationship between tensile strength and size content for a 1000 tex (0.6 Ne) cotton roving [10]. The strength of the unsized roving was 0.2 kg (1.96 N) at a gauge length of 100 mm. These rovings were impregnated in sizing solutions at approximately 90°C, squeezed, and dried at room temperature. Before testing, the samples were conditioned at 20°C and 65% relative humidity. From Fig. 5.9 it appears that, for all sizing agents, a maximum strength of approximately 9 kgf (88.3 N) is attained, which is equivalent to the fiber-bundle strength of the unsized roving [10]. Sodium carboxymethyl cellulose, having good adhesive power, attains this maximum strength at about 3% add-on, whereas those with inferior

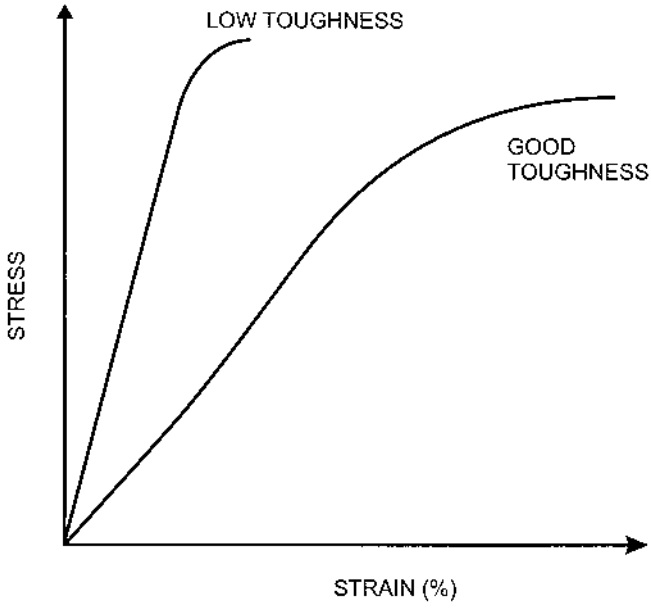

Fig. 5.2 Stress–strain curve of sized rovings at *l* gauge length. (From Ref. 21.)

adhesive power, for example, potato starch, require a higher size add-on ($\sim$ 7%).

The relative differences in the reinforcing abilities of different sizes obtained by such a roving technique, though useful for preliminary screening of different sizing ingredients and size mixtures, are not expected to correlate well with weaveability for obvious reasons. The linear density, fiber arrangement and structure, size add-on, and other sizing parameters in such relatively low twisted rovings are different to those found in actual staple warp yarns subjected to weaving. Besides, the idea of measuring the mere tensile strength of rovings and yarns does not provide effective criteria of estimating weaveability, since no gross differences may be observed between the strength, elongation, or flexibility (of rovings and yarns) before and after treatment with different sizes. Moreover, different weaving efficiencies may be realized with yarns sized with different size mixtures, indicating that the average strength, elongation, and flexibility of most yarns are relatively less important [19].

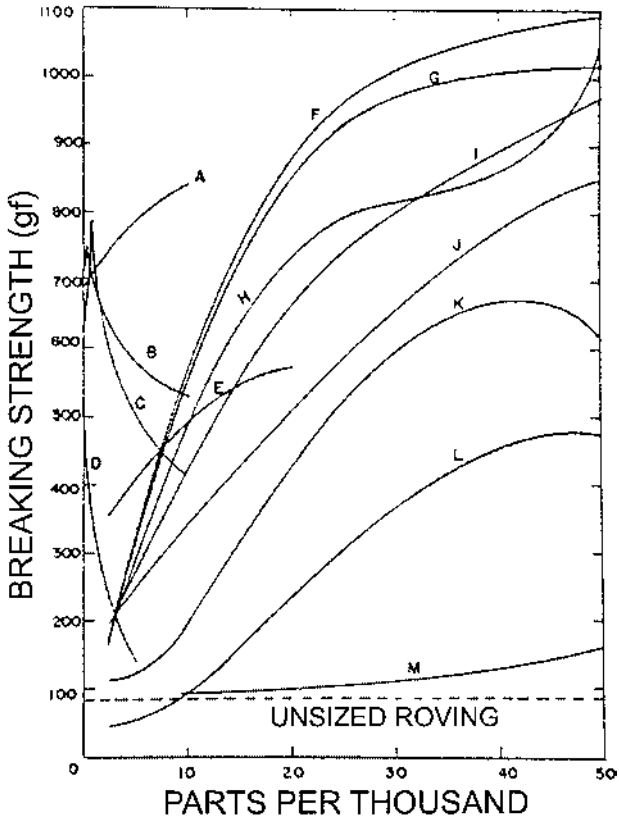

Fig. 5.3 Breaking strength of sized rovings. (A) 2% Clinco 15 + Elvanol 72–51; (B) 2% Clinco 15 + Nopco 1111; (C) 2% Clinco 15 + Onyxsan HSB or 2% Clinco 15 + Onyxsan S50; (D) 2% Stymer S + Nopco 1111; (E) Clinco 15; (F) 25% Stymer S + 75% Elvanol 72–51; (G) Elvanol 72–51; (H) 50% Stymer S + 50% Elvanol 72–51; (I) 75% Stymer S + 25% Elvanol 72–51; (J) Stymer S; (K) Merlon SP; (L) Merlon BR; (M) 0.5% Nopco 1111 + Stymer S. (From Ref. 19.)

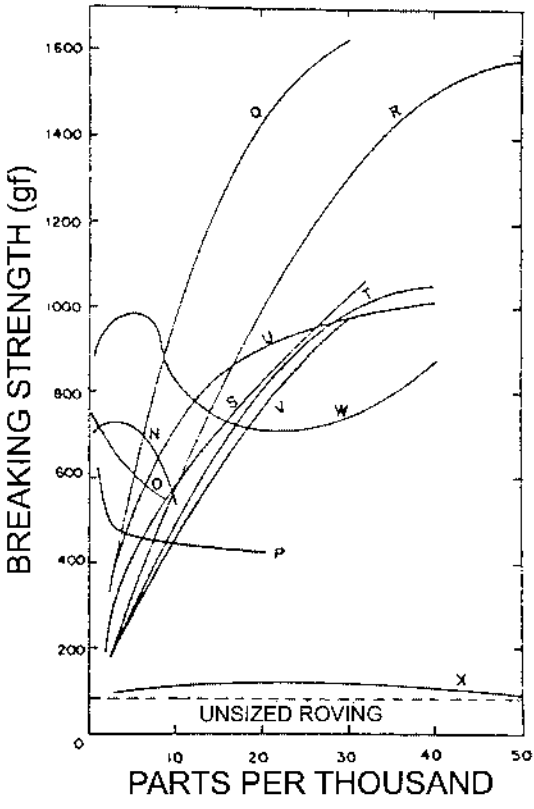

Fig. 5.4 Breaking strength of sized rovings. (N) 2% Cellulosize WP-10 + glycerine; (O) 2% gelatin + Nopco 111; (P) 2% Cellosize WP-10 + Carbowax PF-45; (Q) Methocel, 100 cps; (R) gelatin; (S) 25% Sorbitol + Cellosize WP-10; (T) Cellosize WP-10; (U) Methocel, 15 cps; (V) 100% Sorbitol + Cellosize WP-10; (W) 2% Cellosize WP-10 + sorbitol; (X) Carbowax PF-45. (From Ref. 19.)

5.2.3 Abrasion Resistance

The discussion so far has pertained to the strength and elongation of sized yarns, and no account has been taken of the abrasion resistance of sized yarns. It is known that during weaving the yarns experience the abrasive action of the moving loom parts such as heddle eyes, reeds, whip rolls, and picking elements. Several different criteria of assessing abrasion resistance of sized

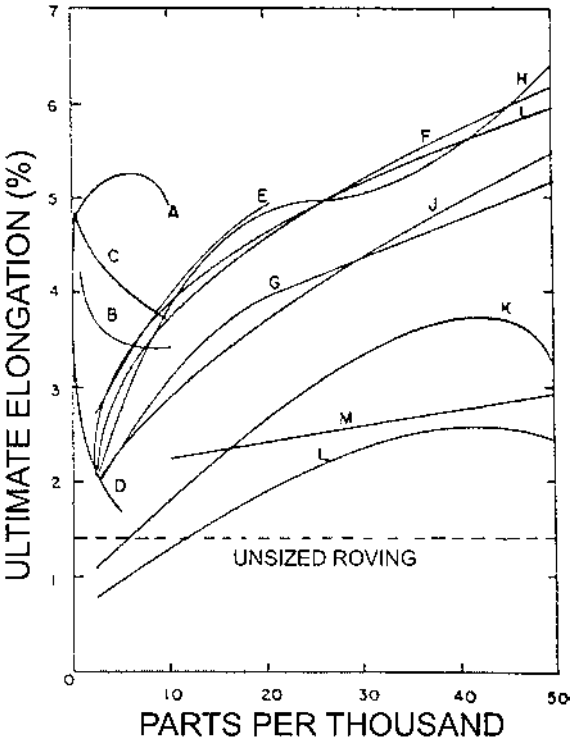

Fig. 5.5 Ultimate elongation of sized rovings. (A) 2% Clinco 15 + Elvanol 72–51; (B) 2% Clinco 15 + Nopco 1111; (C) 2% Clinco 15 + Onyxsan HSB or 2% Clinco 15 + Onyxsan S50; (D) 2% Stymer S + Nopco 1111; (E) Clinco 15; (F) 25% Stymer S + 75% Elvanol 72–51; (G) Elvanol 72–51; (H) 50% Stymer S + 50% Elvanol 72–51; (I) 75% Stymer S + 25% Elvanol 72–51; (J) Stymer S; (K) Merlon SP; (L) Merlon BR; (M) 0.5% Nopco 1111 + Stymer S. (From Ref. 19.)

and unsized yarns have been adopted by a number of research workers [9,22–25]. The comparative improvement in abrasion resistance and strength of the sized yarns due to slashing have been used to correlate with the weaveability [9,22–25]. Owen and Oxley [22] and Owen [23] subjected unsized yarns and yarns sized with various formulations to torsional oscillating stresses on a specially constructed oscillating stress tester [23]. The yarns were sub-

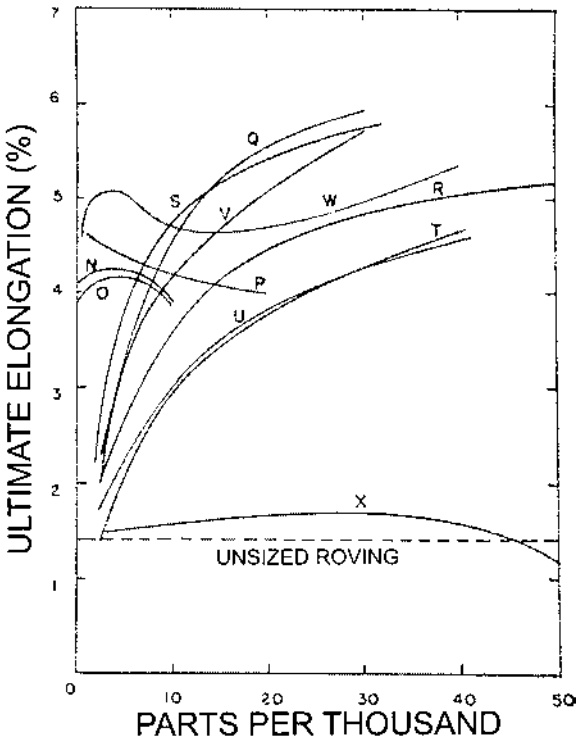

Fig. 5.6 Ultimate elongation of sized rovings. (N) 2% Cellulosize WP-10 + Glycerine; (O) 2% Gelatin + Nopco 111; (P) 2% Cellosize WP-10 + Carbowax PF-45; (Q) Methocel, 100 cps; (R) Gelatin; (S) 25% Sorbitol + Cellosize WP-10; (T) Cellosize WP-10; (U) Methocel, 15 cps; (V) 100% Sorbitol + Cellosize WP-10; (W) 2% Cellosize WP-10 + sorbitol; (X) Carbowax PF-45. (From Ref. 19.)

jected to a fixed number of oscillations, and the results were then expressed in terms of percentage of survivors as shown in Fig. 5.10. The sized yarns clearly performed better than the unsized yarns at all stress levels. Owen [23] used this technique to investigate the effect of sizing from the point of view of resistance to repeated tension variations, similar to those which occur in warp yarns during weaving. Owen and Locke [26] modified the earlier oscillating stress tester [22,23] by incorporating the abrasion element consisting of

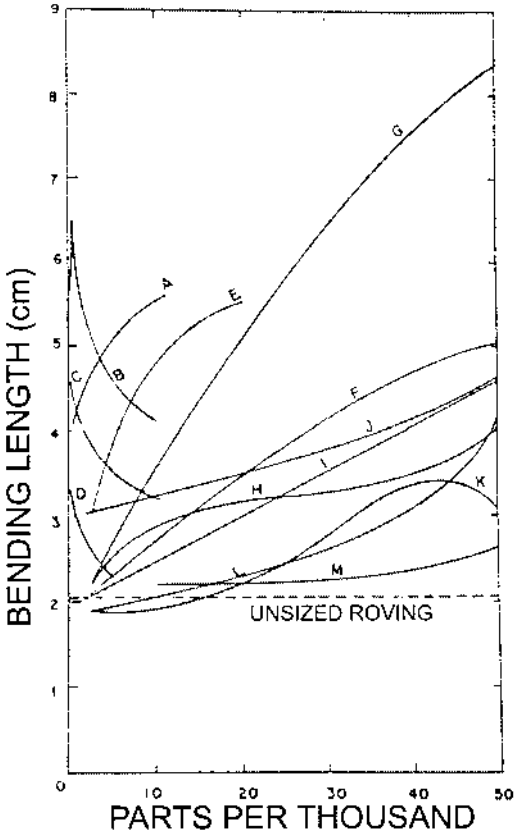

Fig. 5.7 Bending behavior of sized rovings. (A) 2% Clinco 15 + Elvanol 72–51; (B) 2% Clinco 15 + Nopco 1111; (C) 2% Clinco 15 + Onyxsan HSB or 2% Clinco 15 + Onyxsan S50; (D) 2% Stymer S + Nopco 1111; (E) Clinco 15; (F) 25% Stymer S + 75% Elvanol 72–51; (G) Elvanol 72–51; (H) 50% Stymer S + 50% Elvanol 72–51; (I) 75% Stymer S + 25% Elvanol 72–51; (J) Stymer S; (K) Merlon SP; (L) Merlon BR; (M) 0.5% Nopco 1111 + Stymer S. (From Ref. 19.)

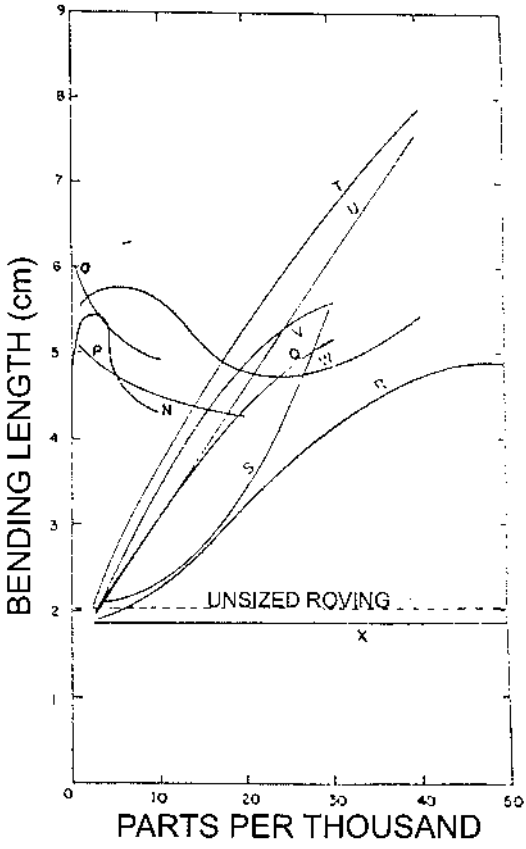

Fig. 5.8 Bending behavior of sized rovings. (N) 2% Cellulosize WP-10 + Glycerine; (O) 2% Gelatin + Nopco 111; (P) 2% Cellosize WP-10 + Carbowax PF-45; (Q) Methocel, 100 cps; (R) Gelatin; (S) 25% Sorbitol + Cellosize WP-10; (T) Cellosize WP-10; (U) Methocel, 15 cps; (V) 100% Sorbitol + Cellosize WP-10; (W) 2% Cellosize WP-10 + sorbitol; (X) Carbowax PF-45. (From Ref. 19.)

three rows of case-hardened steel pegs, as shown in Fig. 5.11. Yarns hanging from the jaws just touch the pegs in the top and bottom rows, and the middle pegs can be traversed sideways to deflect the yarns around by a desired amount. In a test, the yarn hanging from the jaws passes to one side of the corresponding top and bottom pegs and around the opposite side of the displaced middle

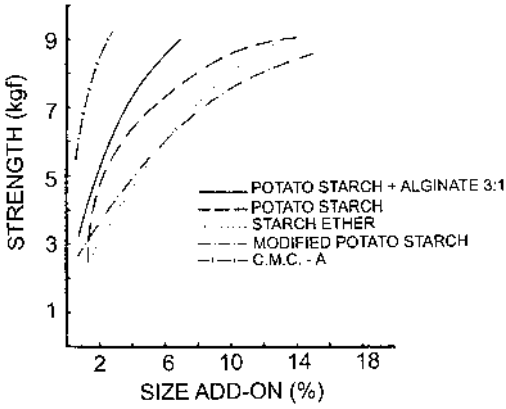

Fig. 5.9 Relation between tensile strength and size add-on of a 0.6 Ne (1000 tex) sized cotton roving. (From Ref. 10.)

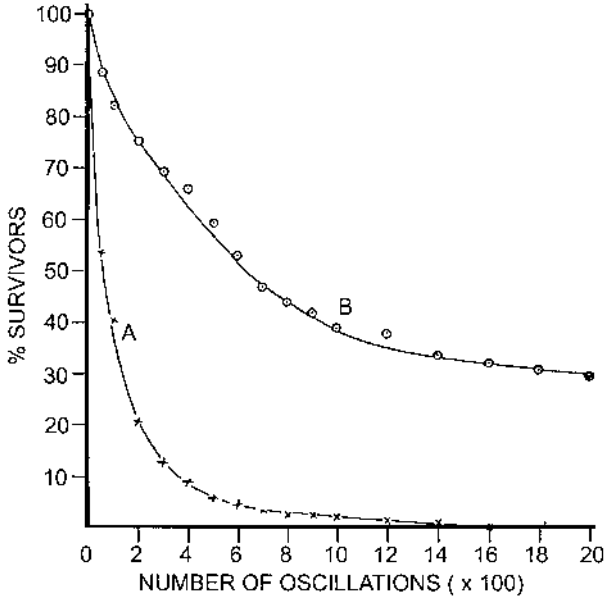

Fig. 5.10 Effect of Torsional Oscillating Stress on Yarns. (A) Unsized; (B) sized with maize starch. Load: 129.6 gf; Speed: 120 rpm. (From Ref. 23.)

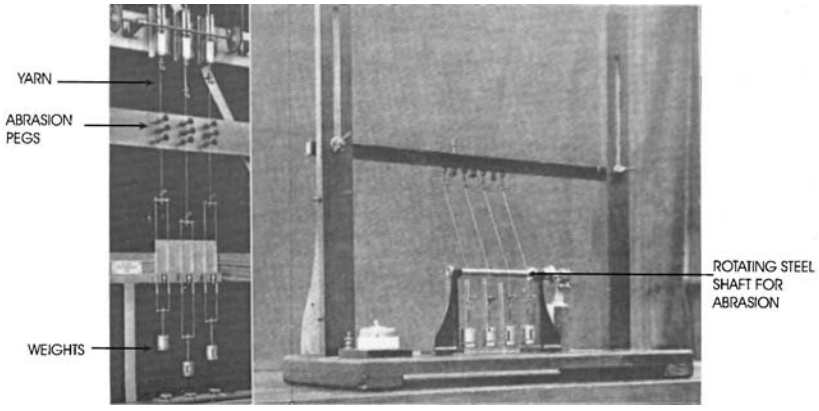

Fig. 5.11 Oscillating stresses abrasion tester. (From Ref. 26.)

peg, and thus abrades the yarn when reciprocated. Owen and Locke [26] also modified the instrument to apply abrasion by the rotating steel shaft, as shown in Fig. 5.11. The shaft was rotated by a belt driven from a small electromotor to provide abrasion to yarns at the point of contact. Using these modified equipment, Owen and Locke [26] subjected yarns to a fixed number of abrasion cycles and measured the breaking strength of such abraded yarns. The results, as shown in Table 5.3, were expressed in terms of percent deterioration in the breaking load, calculated as follows:

$$\text{deterioration}(\%) = \frac{\text{mean strength of yarn before abrasion} - \text{mean strength of yarn after abrasion}}{\text{mean strength of yarn before abrasion}} \times 100$$

They also estimated the resistance of yarns to abrasion in terms of the number of rubs required to break all the specimens in a sample. Typical results of the experimental evaluations are shown in Fig. 5.12 for two experiments, D_1 and D_3, performed at different times but under identical conditions. Because of the arbitrary nature of this test, Owen and Locke [26] concluded that the possibility of predicting yarn performance during weaving was not feasible; however, a comparison of good and bad warp yarns, and of differently sized yarns, could be meaningfully undertaken. Besides the oscillating stresses, the laboratory apparatus did not simulate any other major forces that the yarns experience during weaving.

Table 5.3 Effect of Abrasion Resistance on Breaking Tenacity of Yarn as Measured on Oscillating Stress Machine

Test	Number of rubs	Treatment	Number of breaks in abrasion experiment	Mean breaking load (MBL)	Probable error of MBL	Deterioration (%)	Probable error of % deterioration
1	1000	Unrubbed	—	9.630	0.0918	6.81	1.30
		Rubbed	2	8.974	0.0913		
2	500	Unrubbed	—	9.556	0.0884	5.03	1.23
		Rubbed	0	9.075	0.0827		
3	2000	Unrubbed	—	9.503	0.0892	8.09	1.29
		Rubbed	4	8.734	0.0838		
1a	1000	Unrubbed	—	9.533	0.0830	8.04	1.24
		Rubbed	0	8.767	0.0900		
4	3000	Unrubbed	—	10.013	0.0927	6.61	1.27
		Rubbed	4	9.351	0.0929		
5	200	Unrubbed	—	9.720	0.0922	2.53	1.30
		Rubbed	0	9.474	0.0887		
6	1500	Unrubbed	—	9.883	0.0933	5.76	1.32
		Rubbed	2	9.314	0.0960		
6a	1500	Unrubbed	—	8.873	0.1028	8.64	1.40
		Rubbed	3	8.106	0.0810		
3a	2000	Unrubbed	—	9.107	0.0947	6.09	1.39
		Rubbed	2	8.552	0.0825		

Note: Speed: 120 rpm. Yarns: 5 Ne (118 tex). Number of specimens in each test: 140. Length of specimen: 225 mm (9 in.) Load: 44.7 g.
Source: Ref. 26.

Loom-Action Abrader

In order to find a substitute for full-scale weaving trial—still the most effective method of determining warp yarn performance—earlier researchers have analyzed all the major forces that a yarn undergoes during weaving [27]. Ramirez and Vidosic [27] evaluated the tension variations on a single end for one complete cycle of weaving and also assessed the frictional effects of various loom parts causing longitudinal and lateral abrasion. On the basis of such an experiment, these authors built a laboratory prototype of a loom-action abrader, as shown in Fig. 5.13. Four positions of the harnesses, shown in the figure, were designed to simulate the loom stresses and abrasion that warp yarns

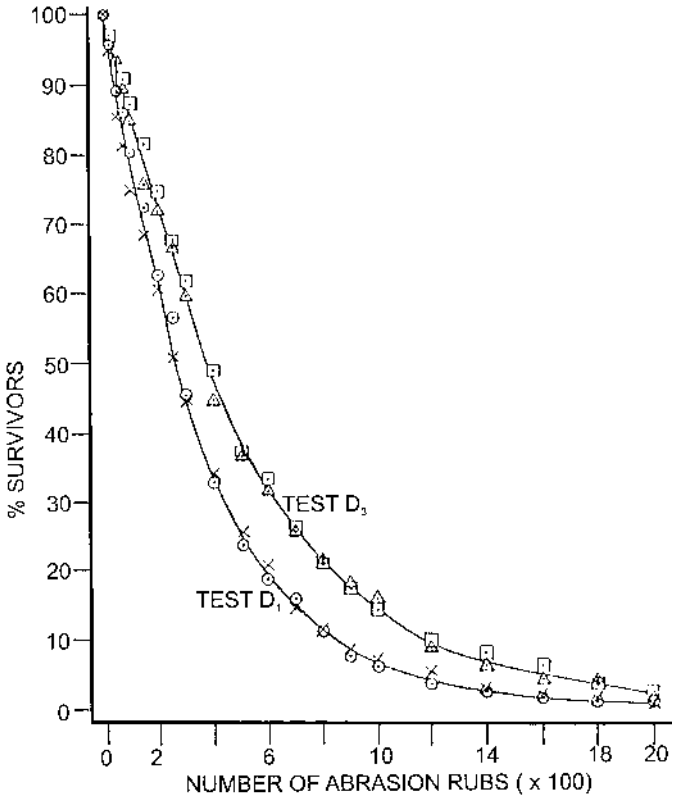

Fig. 5.12 Abrasion resistance of yarns. (From Ref. 26.)

experience on a loom. The forward and backward movement of the reed imposed lateral abrasion on the yarns being tested. The number of cycles required to break the yarns was used as a criterion to characterize the performance of the sized yarns, as shown in Table 5.4. The 22^s Ne (26.84 tex) yarns sized with light, medium, and heavy sizing compounds showed statistically significant differences in their mean number of cycles to break as measured on the loom-action type abrader [27]. A similar approach to the loom-action type abrader [27] was taken by Mehta and Shah [28], who fabricated a dummy loom identical in principle to that used by Ramirez and Vidosic [27]. Instead of a single yarn as tested by Ramirez and Vidosic, Mehta and Shah used a sheet of 250

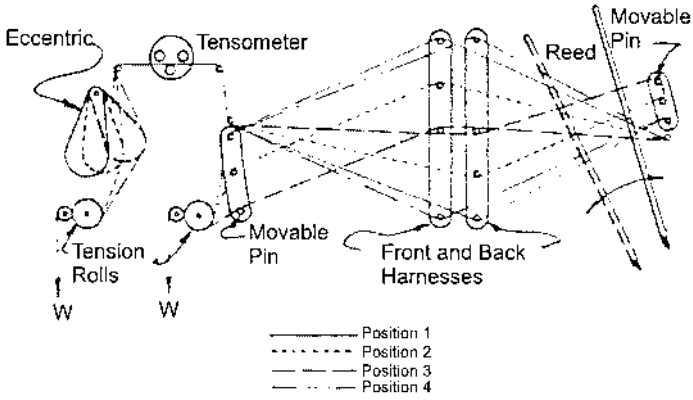

Fig. 5.13 Laboratory abrader with harnesses in four positions. Pins 1 to 4 are fixed; W indicates equal hanging weights. (From Ref. 27.)

to 300 stationary ends of sized warp. The yarns were threaded through a set of heddles and a reed similar to that used on a standard loom. The number of breaks obtained from large-scale weaving trials for the same six samples were compared to those obtained on the dummy loom along with their tensile properties, as shown in Table 5.5. Mehta and Shah [28] calculated rank correlation coefficients between the large-scale weaving trials, tensile strength, breaking elongation, and the data obtained on the dummy loom (Table 5.5). A rank correlation coefficient of 1 was found between breakage rate on the dummy loom and large-scale weaving trials, whereas the correlations obtained with tensile strength and breaking elongation were statistically insignificant. Both the loom-action type abrader [27] and the dummy loom [28] have their own

Table 5.4 Data Obtained on Loom-Action Abrader

Sizing material	Mean number of cycles to break	Standard deviation from mean (%)	Average tensile strength (gf)	Elongation (%)
Light	554	13.5	360	4.9
Medium	651	9.2	340	4.8
Heavy	762	15.4	345	4.6

Source: Ref. 27.

Table 5.5 Warp Breakages and Tensile Properties of Sized Yarns

Sizing treatment	Breaks per 10,000 picks in actual weaving trial	Breaks per 10,000 abrasion on dummy looms	Mean breaking strength (gf)	Mean breaking extension (%)
1	1.5	5.7	269.3	3.5
3	2.7	7.8	286.3	3.6
7	3.8	9.5	292.0	4.3
21	2.2	6.7	311.9	4.9
4	3.2	9.4	263.7	5.4
5	7.2	16.1	263.7	3.0
Rank correlation against large-scale weaving trial	—	1	+0.38	+0.14

Source: Ref. 28.

limitations. The former can test only one yarn, whereas the latter uses a sheet of 250 to 300 yarns but ignores the forward movement of the warp yarns which happens on the loom when the weft thread is subjected to beat-up, resulting in sustained abrasion. Moreover, the dummy loom process is also time consuming; 250 to 300 warp yarns have to be threaded through the heddle eyes and dents of the reed. Obviously, the change to a fresh sample is cumbersome and economically expensive on the dummy loom [28]. Radhakrishnan et al. [29], using this dummy loom [28], measured the tensile properties of sized and unsized yarns before and after sustained abrasion for a fixed number of strokes. The plots of frequency distributions of strength and extension at break for both unsized and sized yarns on a laboratory slasher indicate a pronounced flattening of the distribution for sized yarns subjected to abrasive action, as shown in Fig. 5.14. For laboratory sized yarns, the frequency distribution was found to be bimodal, and this they attributed to a new population of considerably weaker yarns due to sustained abrasive action. Similar experiments repeated on mill sized yarns did not show a pronounced bimodality in the strength of the sized abraded yarns, as shown in Fig. 5.15. However, the considerable flattening of the distribution curve was still visible, which indicated the creation of new weak places [29]. Using a similar technique of assessing tensile strength distribution of sized yarns before and after sustained exposure to abrasive action on a dummy loom [28], Radhakrishnan et al. [29] reported the effect of size add-on on the abrasion resistance of yarns, as shown

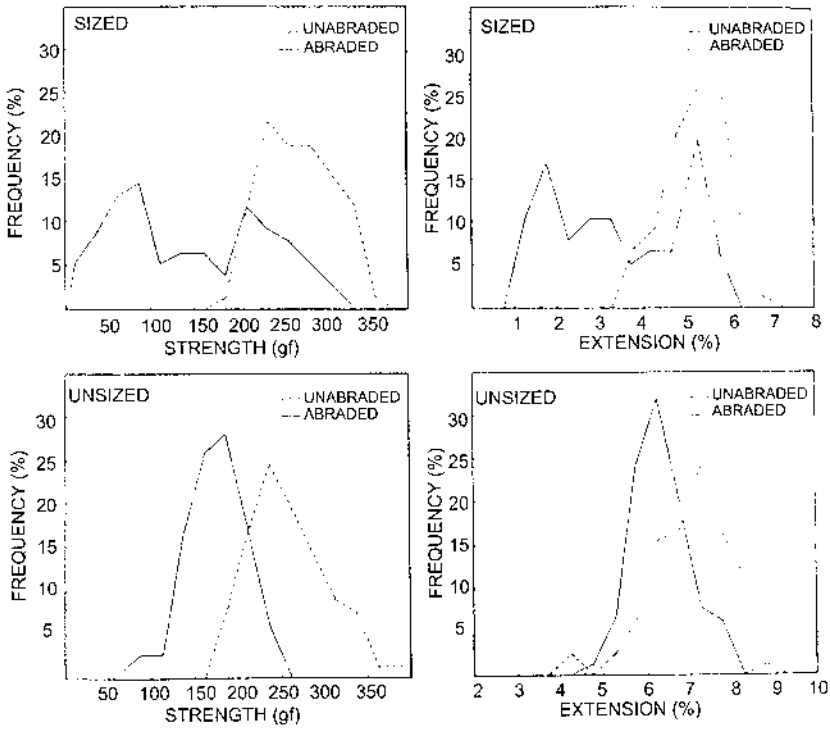

Fig. 5.14 Abrasion resistance of laboratory-sized yarns. (From Ref. 29.)

in Fig. 5.16. Four sets of 100 ends, with 8.8, 7.9, 5.7, and 3.2% size add-on abraded separately for 20,000 cycles on the dummy loom [28], produced 20, 19, 25, and 100 breaks, respectively. A plot of the strength distributions of the survivors, as shown in Fig. 5.16, showed that the characteristic flattening effect increased as the amount of size on the yarn decreased. The authors argued that the bunching of the strength distribution curves of unabraded sized yarns, as shown in Fig. 5.16, did not indicate the superiority of any particular size add-on; however, the strength distribution curves of abraded yarns did indicate differences. Radhakrishnan et al. [29] also evaluated the relationship between the tensile strength distribution of sized yarns that survived the abrasion on the dummy loom [28] and the actual number of weaving breaks, which is shown in Fig. 5.17. The strength of survivors after subjecting yarns to 20,000

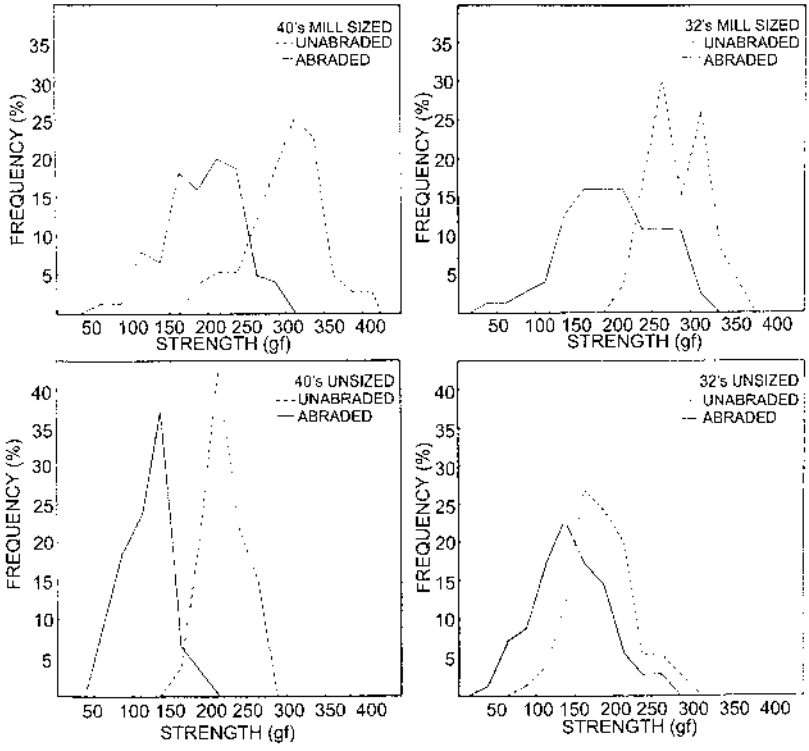

Fig. 5.15 Abrasion resistance of mill-sized yarns. (From Ref. 29.)

abrasion cycles on the dummy loom [28] was plotted in the form of cumulative frequency distributions and was compared with the warp breakage rates per 10,000 picks, as shown in parenthesis in Fig. 5.17. The order of ranking of the extreme left tails of these distributions compared well with the order of ranking of the actual weaving breakage rates.

The sustained abrasion of sized yarns for a prolonged period on the dummy loom [28] created very weak places even though the size film on the yarn provided the needed protection to the core of the yarn. The early rupture and rub-off of the size film exposed the bare yarn surface to the rigorous abrasive action of the heddles and reed of the dummy loom, causing frayed, untwisted, weak places or complete rupture. The places where the applied size adhered cohesively afforded full protection to the yarn or created only a slight

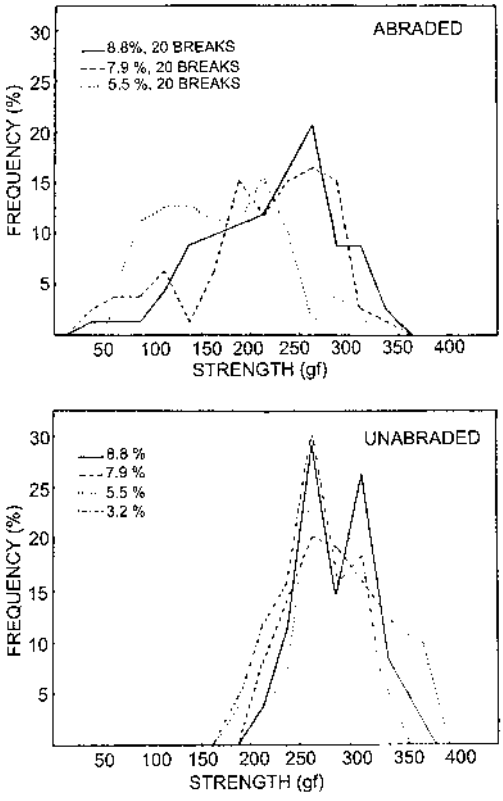

Fig. 5.16 Effect of size percentage on abrasion resistance. Yarns containing less size develop more weak places when subjected to the same amount of attrition in the dummy loom. However, before abrasion has taken place, their tensile strength distributions are much the same. Note particularly the case of the 3.2% size, which gave no survivors after abrasion. (From Ref. 29.)

weakening of the yarn during the course of the abrasive action. When the size film was very irregular, the tendency for local flaking became pronounced, causing superposition of strong and weak places leading to two distinct modes in the bimodal distribution, as shown in Fig. 5.14 [29].

To substitute a large-scale weaving trial by a reliable estimate of weaveability in the laboratory, Ranganathan and Verma [4] fabricated the SRI Weavability Evaluator by incorporating all the features necessary to simulate forces

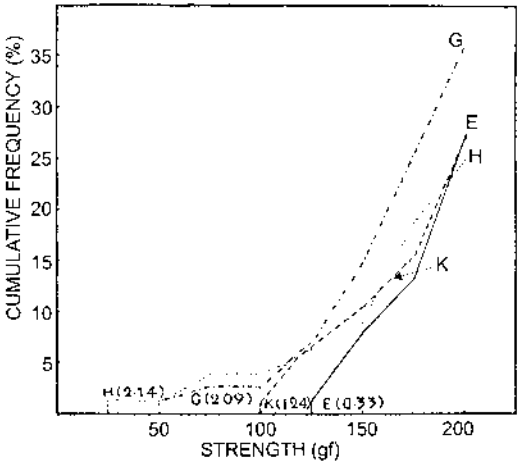

Fig. 5.17 Comparison of different sizes. The yarns E, K, G, and H were sized in four different ways from the same gray lot. They were evaluated by drawing the cumulative frequency curves of strength after attrition in the dummy loom. The position of the extreme left tail of these curves rank the yarn in the same order as the relative warp breakage rates, which are indicated in brackets in the chart. (From Ref. 29.)

acting on a loom. The results of a comparative evaluation between large-scale weaving trials and the laboratory estimate on the SRI Weavability Evaluations are presented in Table 5.6. The laboratory data consistently overestimated the breakage rates for all trials. A similar approach was used to develop the TRS technique for size evaluation [5]. The TRS technique incorporated three steps of operations performed sequentially that consisted of a primary screening phase, a full-scale laboratory evaluation, and an extended mill-scale confirmation trial. The technique, though yielding a high confidence level in predicting the sized yarn performance, was lengthy, time consuming, and expensive to adopt.

Fatigue and Abrasion

So far, no consistent correlation between weaveability and the standard laboratory evaluation of sized yarns in terms of tensile strength/elongation [9–11], elasticity [24], abrasion resistance [4,23,25–29], or adhesion and cohesion of size films [19–21] has been established. This may be due to the fact that

Table 5.6 Comparison of Warp Breakage Rates in the Mill Trials and That Obtained on the SRI Weavability Evaluator

	Breakages in mill		Breakages in SRI laboratory	
Warp yarn	Total number of picks observed	Average breaks per 10,000 picks	Total number of picks observed	Average breaks per 10,000 picks
80s	2×10^5	1.0	2.3×10^5	2.04
34s	2×10^5	2.1	1.5×10^5	4.10
18s	2×10^5	3.47	2.7×10^5	8.23

Source: Ref. 4.

during the actual weaving process the warp yarns are subjected to cyclic stresses that are complex in nature; these include cyclic tensile, bending, and torsional stresses. The resistance of a yarn to such repeated stresses, called fatigue strength, was considered by Faasen and van Harten [10,11] and by Owen and Oxley [22]. Figure 5.18 shows a plot of the relation between the size content, the static strength, and the fatigue strength of a warp yarn. The fatigue strength of the unsized yarn is only 40% of the static strength. Even

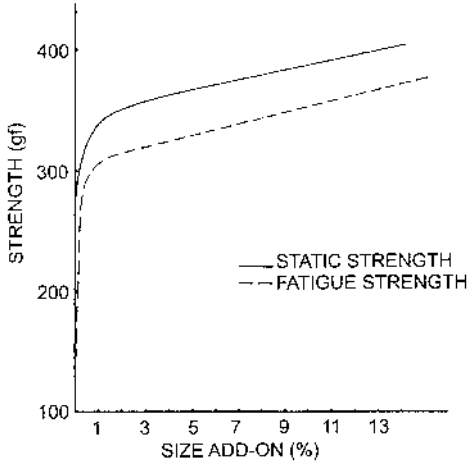

Fig. 5.18 Effect of size add-on on static and fatigue strength. (From Ref. 10.)

with a very low amount of size, less than 0.5%, the fatigue strength of the sized yarn equals the static strength of the unsized yarn. Upward of size content of 1%, the fatigue strength and the static strength increase linearly with an increase in size content; however, the fatigue strength is around 80% of the static strength [10]. Faasen and van Harten [10,11], however, suggested that ''since the weaving tension, in general, is no more than 20% of the static strength of the unsized yarns, neither the static strength nor the fatigue strength is an important factor in the assessment of the properties of sized yarns. It is, therefore, necessary to find other criteria to determine the weaveability of sized yarn.''

The actual weaving process is far more complex than what is envisaged in laboratory evaluations. The warp yarn is subjected to complex mechanical actions consisting of cyclic extension, abrasion, and pseudotwisting – untwisting due to extension and bending. The warp yarns under the state of dynamic loading on a loom have to withstand cyclic stresses imposed due to the lifting of heddles, flexure and buckling in the heddle eyes, and frictional forces arising due to the abrasion of yarns with heddle eyes, reed wires, whip roll, drop wires, and the picking element [10,11,30–32]. It is also obvious that maximum chaffing takes place in the heddles because a force normal to the heddle eye is set up due to the deflection of the yarn and its movement in a plane perpendicular to the plane of the eye, which in turn intensifies the rubbing action [32]. The forward displacement of warp yarns during beat-up and the extension of the yarns during shedding should be accounted for as the reed and the pick being moved to the fell of the cloth exert a rubbing action on the warp yarns. In shuttle looms, the bottom part of the shed frequently rubs against the sley board, and also the shuttle abrades the warp yarns during its traverse both in the longitudinal and the transverse directions. The abrasive action is further intensified by the sett of the cloth being woven; increase in warp and weft density increases abrasion and the resultant warp yarn tension [32]. The combined effect of all these complex deformations causes the yarns to become more hairy, and if sizing is not done adequately the resultant hairiness causes the yarns to entangle and break during the weaving action. It is extremely difficult to quantify this aspect of warp breakage and to establish a correlation between laboratory measurements and actual warp yarn performance. The yarn breakage due to hairiness needs to be studied extensively if any further understanding of the warp yarn performance during weaving is to be properly accounted for.

Zolotarevskii [32] studied the effect of abrasion and repeated extension on unsized and sized yarn. He showed that repeated extension without abrasion had no effect on yarn strength, as shown in Table 5.7, while even partial

Table 5.7 Effect of Repeated Extension on Warp Yarn Strength

	Breaking strength of sized yarn	
	gf	%
From warp beam	277.1	100.0
Warp-beam to pulsator	277.0	100.0
Warp-beam to abrader	253.8	91.7
Warp-beam to pulsator to abrader	239.3	86.4
Extracted from fabric	258.2	93.2

Source: Ref. 32.

abrasion caused a decrease in strength by 8.3%. The partial abrasion of yarns following the process of repeated extension loading on a Borodovskii pulsator [33] resulted in a decrease in strength of the warp yarn by 13.6%. This implied that the repeated extension by itself (below the endurance limit) did not impair yarn strength but almost doubled the loss in strength when repeated extension and abrasion were combined. Zolotarevskii [32] concluded ''repeated extension has an indirect but highly adverse effect, in that it decreases the resistance of warp yarn to abrasion. During weaving, the loss in strength of the warp yarn is caused by abrasion only.'' However, Zolotarevskii did not examine the effect of subjecting the warp yarn to both fatigue and abrasion simultaneously. Milovidov [34] performed cyclic tension tests on a Borodovskii pulsator [33] at 350 cycles/min on unsized yarns having preset relative deformations of 0.75, 1.0, and 2.0% and sized yarns at 1.0 % extension. He reported that sizing improved the yarn endurance to cyclic loading, defined as the number of cycles to break. The increase in endurance strength was far greater than the increase in breaking strength. He further subjected three yarns spun at different twist levels to the endurance test and compared them to the end-breakage rate on ten looms recorded over a period of 3 months. The results are summarized in Table 5.8. The results show that the yarns with the highest endurance and twist have the lowest end-breakage rate, even though their breaking strength is the lowest. The yarn having the lowest twist shows the highest end-breakage rate despite its highest tensile strength. Milovidov [34] calculated the coefficient of correlation, r, between the end-breakage rate on the looms and the endurance of the sized warp yarns ($r = -0.890$), breaking strength of sized warp yarn ($r = -0.36$), and the extension of the sized warp yarn ($r = -0.72$).

Table 5.8 Relation Between End-Breakage Rate and Endurance, Breaking Strength, and Elongation at Break of Sized Warp Yarn

Twist variant	Coefficient of twist (α of the warp yarn)	Total length tested (m)	End breaks per zone: Between backrest and heald shaft	End breaks per zone: Between heald shafts and reed (in back position)	End breaks per zone: Between reed and fell of cloth	Total end breaks	End breaks per meter of cloth
3	123	170	22	21	3	46	0.27
4	150	170	23	13	1	37	0.22
5	165	170	14	8	3	25	0.15

	Test variants: III		IV		V	
Indices	Unsized	Sized	Unsized	Sized	Unsized	Sized
Actual count (tex)	54.1	52.1	52.2	51.6	52.2	51.6
Breaking strength of single yarn (g)	202 ± 8	249 ± 7	218 ± 9	235 ± 10	210 ± 9	234 ± 10
Breaking extension (%)	4.4	3.7	4.7	3.8	4.9	4.4
CV of breaking strength (g)	14.4	10.2	14.5	14.9	14.5	15.8
Endurance under cyclic extension (cycles to failure)						
Unsized yarn	1325 ± 368		2316 ± 805		3347 ± 504	
Sized warp		1653 ± 606		3019 ± 253		5070 ± 270
End breaks in spinning per 1000 spindle/hour	140	—	111	—	95	—

Source: Ref. 34.

Davydov et al. [35] studied the residual strength of cotton yarn of 18.5 tex at a constant cyclic speed, base loads, and sample lengths but at different numbers of cycles. The results obtained indicated that the cyclic extension produces changes in the initial pattern of yarn strength distribution. The changes in the yarn section which resulted from repeated extension vary with the yarn sections. The largest changes occur in the ''weaker'' sections where the probability of yarn rupture steadily increases. In the ''strong'' sections of the yarn, the repeated extension produces practically no variations in the yarn strength [35].

Fatigue

The repeated loading and unloading of a material under small stresses (whether in repeated uniaxial, bending, or shear) often causes cumulative extension, which decreases its resistance to failure despite the stress intensity being well below the ultimate strength under static load. Such a phenomenon is commonly known as fatigue. The initiation and propagation of such cumulative fatigue damage is hard to detect in practice, and generally there is no prior indication of the impending failure [36]. It appears, therefore, that the yielding of warp yarn during weaving is perhaps independent of the yarn strength and abrasion resistance of the individual yarns but depends on the gradually diminishing resistance of the material attributable to the cumulative damage inflicted due to tensile fatigue under relatively small forces (well below the breaking point applied under a static load) combined with abrasion [34,37,38]. The studies on fatigue resistance of staple and multifilament yarns are of great importance as fatigue affects the processing performance, for example, the behavior of sized yarns during weaving and that of multifilament yarns in automobile tires.

The assessment of fatigue damage under cyclic tensile and bending forces accompanied by abrasion may be made according to the following three criteria [37]:

1. *Failure*, in which the yarn is subjected to fatigue until it fails under cumulative damage. The results obtained, usually in terms of fatigue cycles, are expressed as fatigue lifetime or survival time. In this criterion only information about lifetime is available; the rate at which the yarn performance deteriorates with the increasing intensity of fatigue is not known. Obviously predicting the impending failure is not possible by this method.
2. *Loss in mechanical properties*, where the yarn is subjected to a known number of cycles prior to its fatigue lifetime and the results are expressed in terms of loss in some mechanical properties, usually

tensile. If the yarn is subjected to a known number of cycles in a progressively increasing order and the loss in mechanical properties is estimated at each such step, then the rate of fatigue damage can be assessed. The rate of fatigue damage yields useful information about practically unacceptable levels of deterioration in yarn properties. The yarn, though not broken, may have poor residual properties after a certain number of fatigue cycles. Such a yarn with decreased resistance may be prone to potential failure.

3. *Visual damage*. The previous two criteria are objective in nature, whereas this method of assessing fatigue yields only qualitative information about the pattern and extent of fatigue damage inflicted on the fine structure of the yarn. The fiber damage resulting due to fatigue can be visualized to understand the fatigue resistance of different types of fibers.

Reutlinger Webtester

To alleviate the attendant risks and cost of time consuming weaving trials, therefore, an instrument that can simulate all the important stresses occurring during weaving should be selected. The Sulzer-Ruti Webtester, similar in principle to that designed by the Institute of Textile Technology, in Reutlingen [39,40] is shown in Fig. 5.19. This apparatus simulates all the most important stresses to which the yarns are subjected during weaving. The important weaving forces and the manner in which they are simulated on the webtester are described in Table 5.9 [41]. The base or pretension on the webtester simulates the static warp tension on the loom, which is applied by hanging predetermined deadweights while mounting the specimens. The extent of the sinusoidal motion of the yarn clamp determines the strain amplitude, which simulates the cyclic extension imposed due to the lifting of the heddles. The abrasion on the yarn due to the rubbing with heddles and reed is simulated by the abrasion element consisting of pins. The yarn bending and buckling in the heddle eyes are simulated by deflecting the specimens around the abrasion pin. The speed of fatiguing on the webtester, expressed as cycles per minute, simulates the speed of weaving. The intensity of the various forces listed in Table 5.9 can be varied within a realistic range in various combinations to simulate practical conditions similar to those that occur on a loom.

The webtester is connected to a microprocessor to which all signals are fed after the corresponding analog/digital conversion. The measured data are cyclically sampled and processed continuously. The data on calculated properties such as breaking strength, breaking extension, and work of rupture are available at the end of the test in addition to other statistical calculations.

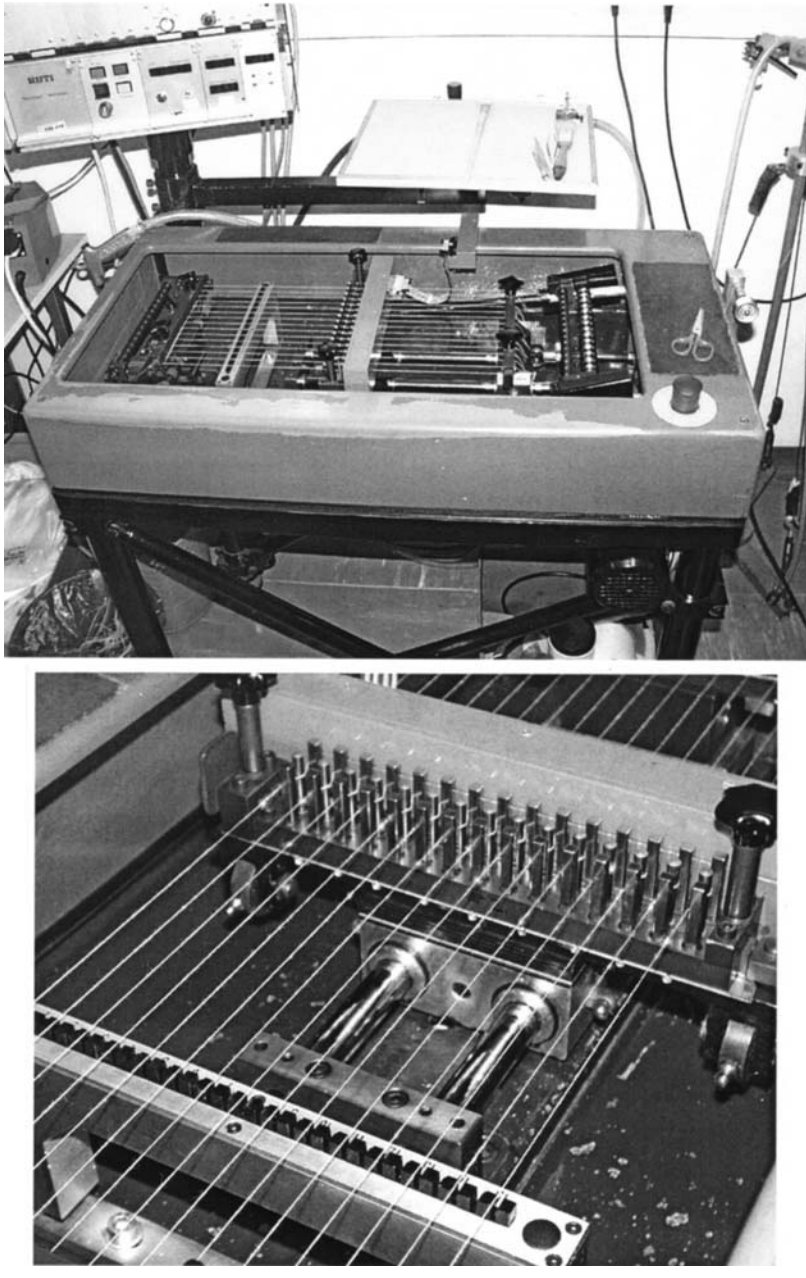

Fig. 5.19 Reutlingen Webtester. (Courtesy of ITV Denkendorf.)

Table 5.9 Weaving Stresses and Analogous Simulation on the Webtester

Forces during weaving	Analogous forces on the webtester
Static warp yarn tension in center of the shed	Initial stressing force by application of weights while mounting specimens
Cyclic extension through lifting of healds	Cyclic extension through sinusoidal motion of yarn clamps in axial direction
Abrasion on yarn due to healds and reed	Axial abrasion through abrasion element consisting of pins
Bending and buckling in heald eyes	Bending and buckling around abrasion pins
The level of tension is maintained by warp-beam regulator	The initial base tension is measured in the test and maintained constant during the test

Source: Ref. 41.

A line diagram of a set of yarn specimens mounted on a webtester is shown in Fig. 5.20. On the webtester, 15 yarn specimens, each 50 cm long, are mounted under constant base tension between two clamps. One clamp is fixed and the other clamp is movable horizontally in the plane of the mounted specimens to impose predetermined cyclic extensions simultaneously to all 15 yarn specimens. The yarns are deflected around stationary abrasion pins made of brass or any other material at a fixed setting. There are two sets of pins on the webtester: two square pins are mounted on a fixed plate and the center pin—circular in cross section—is mounted on a movable plate so as to adjust the penetration of the pin to a desired level of bending and abrasion intensity. Figure 5.21 shows the schematic of the abrasion pin configuration on a Sulzer-Ruti Webtester [42]. The yarn samples are then subjected to cyclic extension at a predetermined speed. With the progressively increasing fatigue action, the yarn breaks and the number of cycles at break are recorded by the microprocessor. The breakage of any one of the 15 specimens necessitates that the total base tension under which the remaining specimens are mounted must be reduced accordingly by an appropriate amount so as to maintain a constant base tension throughout testing. This is automatically achieved by the microprocessor on the Sulzer-Ruti Webtester as the rupture of the specimen is recorded. The test is usually continued until 10 out of the 15 yarn samples have ruptured. It is important to note that due to the imposed cyclic tensile fatigue on the yarn samples some yarns elongate and develop slack. Such slackened yarns exhibiting negligible tension no longer experience the cyclic

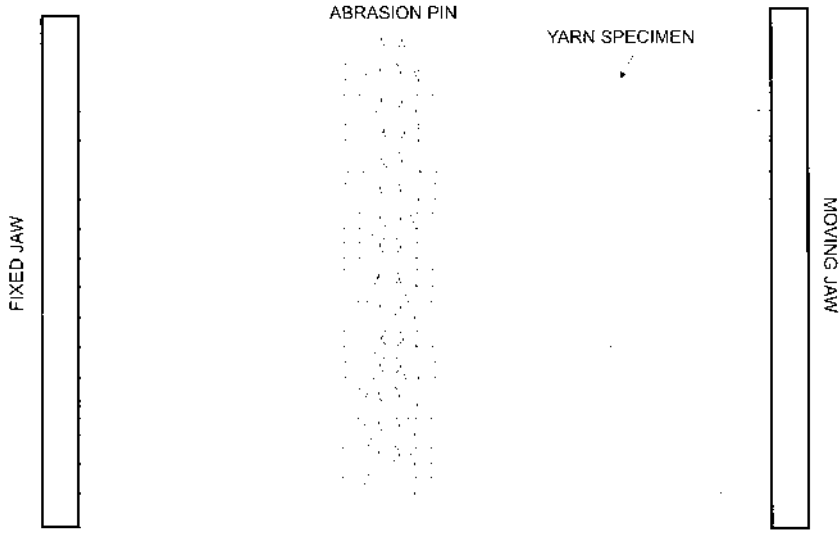

Fig. 5.20 Line diagram of mounted specimens on a webtester.

fatigue and abrasion action. Under practical weaving conditions, such slackened yarns have no serviceability, and therefore during fatigue testing such an occurrence is classified as a pseudobreak. The yarns are then manually removed, with the cycles at which the yarns slackened being recorded. On a recent Reutlinger Weaving Tester, photoelectric devices are fitted to monitor the slub formation due to abrasion and slackening of yarns due to fatigue. The signals from photoelectric sensors are transmitted to the microprocessor for automatic registration of slub formation and slackening of the yarns during the test.

To understand the rate of fatigue damage in yarns, it is necessary to know the fatigue lifetime of the yarn based on the failure criterion. The rate of fatigue damage can be conveniently estimated by subjecting yarns for a known number of fatigue cycles on a time-scale of zero to the maximal value of the fatigue lifetime determined on the basis of failure. Then the fatigue results can be represented in terms of loss in some important yarn property, for example, tensile strength. Anandjiwala and Goswami [37] have reported a study in which they subjected staple yarns to fatigue cycles equal to 25, 50, 75, and 100% of their fatigue lifetimes estimated on the basis of failure. The yarns that survived the imposed fatigue were collected and mounted on

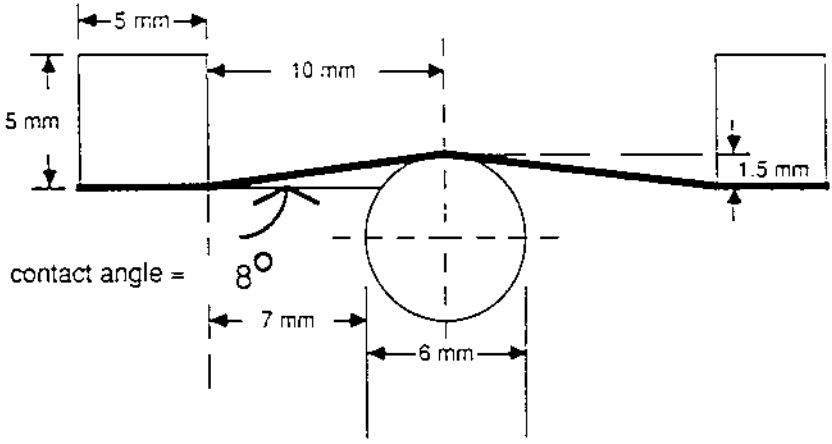

Fig. 5.21 Schematic diagram of the webtester abrasion pin configuration. (From Ref. 42.)

a black board. These survivors were in turn broken on an Instron tensile testing machine at a gauge length of 25 cm. At least 30 such survivors were collected at each level of fatigue. The yarns were mounted between the jaws of an Instron tensile tester such that the abraded portion remained in the center. The results were then expressed in terms of tenacity and elongation at break. For visual observation of fatigue damage inflicted, the yarns were observed with a scanning electron microscope.

Analysis of Fatigue Results

The discussion presented in the following sections on analysis of fatigue is primarily based on numerous studies carried out by various authors [39–42,45,49–55,57–61,63–67] whose work is referenced in the text when quoted. The earlier attempts to characterize fatigue performance of various materials, including textiles, were made in terms of average, median, or logarithmic lifetimes [39–41,43–45]. Following these early experimental findings, statistical development in the area of extreme value theory [46] and its application to fatigue phenomenon of various metals was first reported by Weibull [47]. Following the developments in engineering materials, research workers in textiles have shown that the cyclic fatigue behavior of fibers [48–52], yarns [53–58], tire cords [59–61], and fabrics [62] generally follow the third asymp-

totic distribution of extreme value theory [46], commonly termed the Weibull distribution. However, research findings are inconsistent, especially concerning the fatigue performance of fibers and yarns, in predicting the performance of sized yarns during weaving. The problem is in the understanding of the exact nature of the distribution and how it can help in discerning the mechanism of fatigue performance of fibers and yarns.

Prevorsek and Lyons [52] have identified both unimodal and bimodal distributions for acrylic fibers. They have shown that the distribution changes from unimodal to bimodal with the increase in stroke from 2.0 to 4.1% at 250 cycles/min [52]. For nylon and polyester fibers, they have confirmed that the unimodal pattern of the distribution is well suited with only some exceptions [51,52]. The controversy of observing unimodal and bimodal distributions for the tensile fatigue behavior of yarns have been extensively reported and discussed by various researchers [57,58,63–68]. The earlier studies of the tensile fatigue of yarns have reported bimodal distributions of fatigue lifetimes [63]; however, later studies have shown the preponderance of a unimodal Weibull distribution [56,57,64]. This poses a formidable problem in understanding the mechanism of yarn failure under cyclic tensile loading since the mechanism involved in bimodal behavior is inherently different to that in a unimodal Weibull distribution.

Failure Criterion. Trauter and his coworkers [39–41] utilized the Reutlinger Webtester to measure the number of cycles to break when yarns were subjected to abrasion and fatigue. They continued testing until 9 out of 15 specimens were broken or slackened as per the method described in the previous section. They replicated the test four times, giving a total 60 yarn specimens tested. They recorded number of cycles at break for first nine breaks and for four replications, as shown in Table 5.10. From this test they obtained mean values ST(1) to ST(9), as shown in Table 5.10, and transferred them on to a semi-logarithmic plot, as shown in Fig. 5.22. This produces either a straight line or nonlinear curve which can be converted into two straight lines. This plot on a semi-logarithmic scale was designated as a ''life characteristic curve,'' and it was used to characterize the abrasion resistance of the yarns tested. The authors further simplified the analysis by considering the number of cycles at break for the first and sixth yarn break, denoted by ST(1) and ST(6), respectively. By using this simplified analysis, Trauter and his coworkers [39–41] explored the effects of the test conditions and sizing parameters.

The fatigue lifetimes of all 150 specimens of 20 tex, 50/50 cotton/polyester ring-spun yarns that failed are shown in Fig. 5.23 by Anandjiwala and

Table 5.10 Typical Test Results on the Webtester

Sequence of yarn break	Number of Cycles at Break (ST)				
	Trial 1	Trial 2	Trail 3	Trail 4	Average
1	522	480	515	532	ST(1) = 512
2	735	678	702	723	ST(2) = 709
3	975	1041	1023	988	ST(3) = 1006
4	1093	1131	1082	1145	ST(4) = 1113
5	1188	1255	1209	1153	ST(5) = 1201
6	1301	1452	1435	1409	ST(6) = 1399
7	1478	1402	1532	1522	ST(7) = 1483
8	1631	1693	1732	1746	ST(8) = 1701
9	1742	1780	1861	1832	ST(9) = 1804
Yarn elongation ΔL (mm)	1.54	1.36	1.61	1.45	1.49

Note: ST(1) and ST(6) represent the abrasion characteristics (number of cycles for the first and sixth yarn breaks).
Source: Ref. 39.

Goswami [37]. The range of the number of cycles at break varies from a minimum of 1903 to a maximum of 4076, the calculated average lifetime being 3055.8 cycles, with a standard deviation of 568.9 cycles. A histogram of the data is plotted in Fig. 5.24 [37]. The distribution obtained is far from normal in nature. Representing such widely scattered data in terms of average lifetimes will not exactly characterize the complete phenomenon of fatigue.

The problem of analyzing such nonnormal asymmetric distributions that occur in fatigue experiments has been considered and discussed at length by several authors [45–47] under the broad spectrum of extreme value statistics. Based on such extreme value statistics, some researchers have fitted various statistical distributions, such as the first asymptotic, the log-normal and the third asymptotic distribution (commonly known as Weibull) [46,47]. Barella [63–65], Prevorsek et al. [45], and Picciotto and Hersh [57] have shown that the fatigue behavior of yarns under cyclic extension accompanied by abrasion resistance follows the three parameter Weibull distribution, with some exceptions. However, these authors have reported somewhat inconclusive results in terms of the unimodal and bimodal pattern of distribution.

The Weibull distribution of the extreme value theory is given by

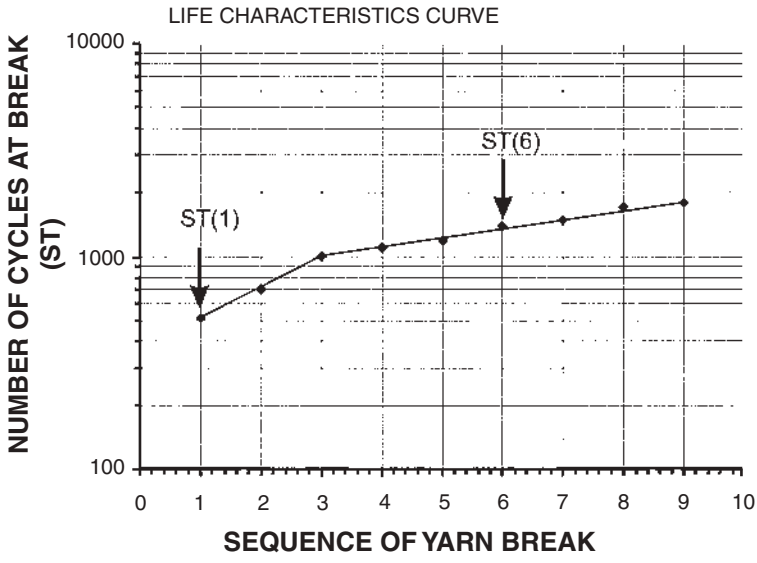

Fig. 5.22 Life characteristics curve of yarn subjected to fatigue on the webtester. (From Ref. 39.)

$$P(x) = \exp\left[-\left(\frac{x - x_o}{v - x_o}\right)^k\right] \quad \text{for } x \geq x_o, v \geq x_o, \text{ and } k > 0 \tag{5.1}$$

where $P(x)$ is the probability that the yarn will survive x cycles; x_o is the lower bound of the distribution, known as minimum lifetime, that all specimens are expected to survive; v is the characteristic extreme lifetime; and k is a scalar parameter that determines the shape of the distribution. Among several different methods of estimating Weibull parameters [46,47], it has been shown by Picciotto and Hersh [57] that the linear regression technique produces the most plausible results. Consequently, the Weibull distribution may be expressed in a more convenient linear form by double logarithmic transformation of Eq. (5.1) to give

$$\ln\left\{-\ln\left[P(x)\right]\right\} = y = k \cdot \ln(x - x_o) - k \cdot \ln(v - x_o) \tag{5.2}$$

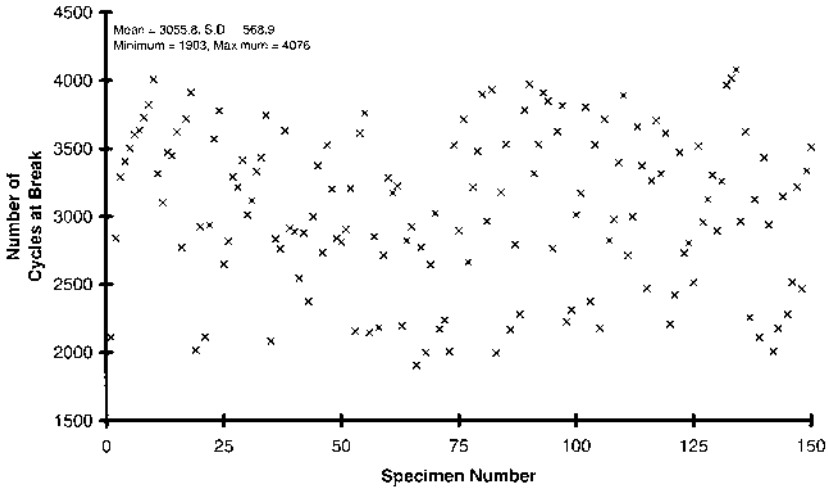

Fig. 5.23 Diagram of typical fatigue behavior based on failure criterion. (From Ref. 37.)

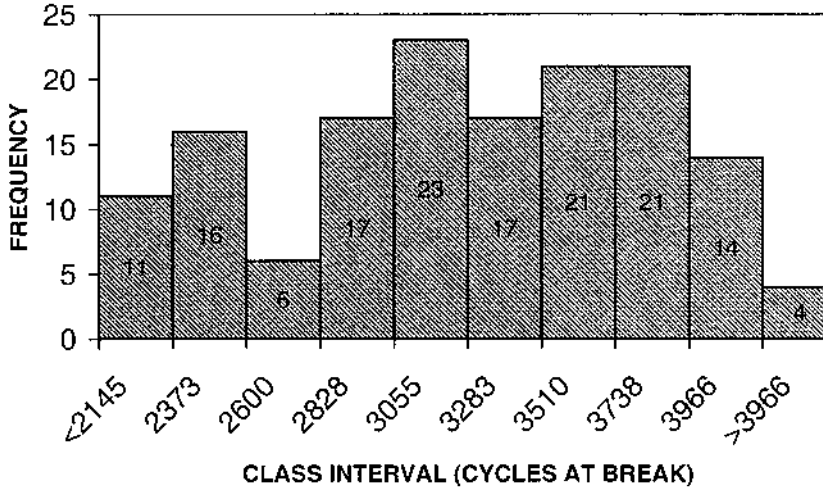

Fig. 5.24 Histogram representing typical fatigue results based on failure criterion. (From Ref. 37.)

The survival probability may be estimated by using a standard computational program [69] which uses the method of maximum likelihood as described by Kalbfleisch and Prentice [70]. Figure 5.25 shows the probability of survival plotted against the number of cycles at break, which is similar to that plotted by other authors [44,46,47,64]. The estimation of Weibull parameters x_o, v, and k, for a given N experimental observations, can be conveniently carried out by defining a function S such that

$$S(x_o, v, k) = \sum_{i=1}^{N} (y_i - y_{ic})^2$$

where the subscript c indicates the computed values for some approximate initial guesses of x_o, v, and k. When S becomes zero, separate residue is also zero. The problem of changing the initial guesses until S, which is a function of these guesses, reaches a minimum value (ideally zero) can be solved by a standard function minimizing technique [71]. A computer program was prepared for fitting the Eq. (5.2) and to estimate all three parameters for given experimental results [37]. A typical fit based on Eq. (5.2) for the data plotted

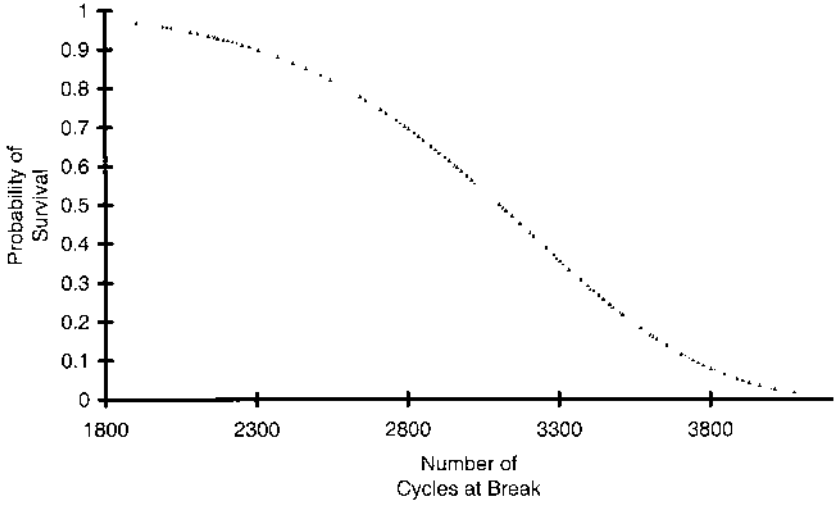

Fig. 5.25 Typical plot of number of cycles to break versus probability of survival. (From Ref. 37.)

in Figs. 5.23 and 5.25 is shown in Fig. 5.26. The estimated parameters of the Weibull distribution are $x_o = -0.054$, $v = 3289.014$, and $k = 6.3724$, with coefficient of determination (r^2) of 0.999 [37].

Rate of Fatigue Damage Criterion. The rate of fatigue damage in fibers and yarns has been ignored by various research workers [50,51,57,64]. The idea of fatigue lifetimes only on the basis of failure criterion, discussed in the previous section, is hardly enough to characterize the complete fatigue behavior of yarns and its anticipated effect on weaveability, since the characteristic lifetimes calculated by fitting the Weibull distribution are sometimes far higher than the actual tensile fatigue cycles imposed on looms [42]. Even the mean lifetimes used as a criterion to describe the fatigue failure of yarns [44] is also often several times higher than the actual level of tensile fatigue experienced by yarns during weaving. This implies that the reported breaks of such yarns during actual weaving perhaps occur well before the imposed fatigue attains the value equal to its characteristic lifetime. Therefore, the understanding of the progressive deterioration of important yarn properties, for example, tensile strength, at increasing fatigue level may yield useful information about the possibility of potential failure. This may in turn contribute toward estimating

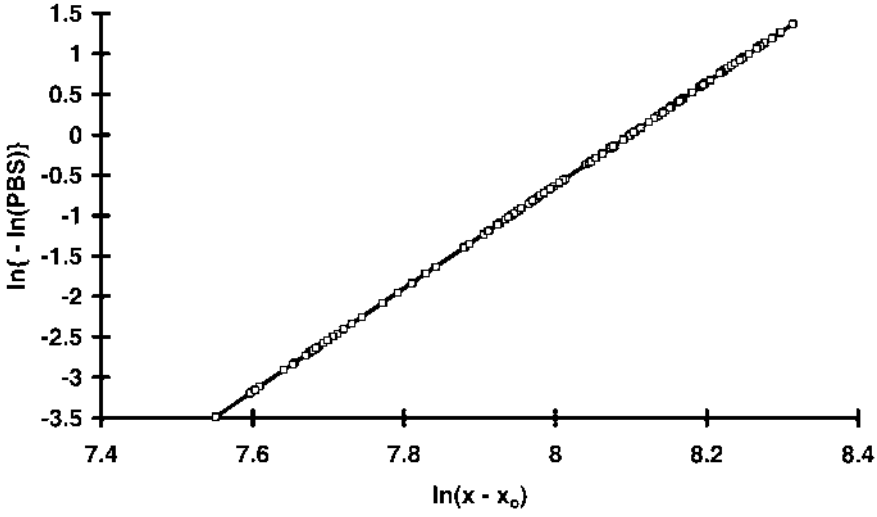

Fig. 5.26 Typical fit of three-parameter Weibull distribution to experimental results. (From Ref. 37.)

the capacity of the material to sustain failure and the phenomenon of impending failure which is otherwise not very well understood.

Figure 5.27 shows a typical graph of loss in tenacity and elongation at break with increasing fatigue. Values of tenacity and elongation at break marked at 0% of the characteristic lifetime indicate the properties of yarns before being subjected to fatigue. In general, as the fatigue level is increased in steps of 25, 50, 75, and 100% of the characteristic fatigue lifetimes, the tenacity and elongation at break decrease. The extent of change in tenacity

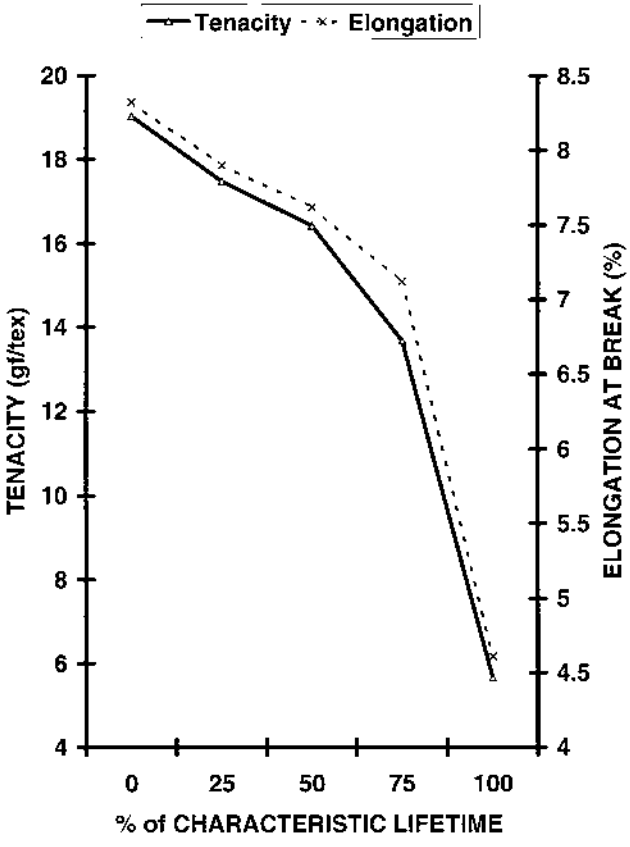

Fig. 5.27 Plot of typical fatigue results based on rate of damage criterion. (From Ref. 37.)

and elongation at break for each level of fatigue is calculated and given in Table 5.11. In this particular test, the deterioration of the yarn properties is relatively small up to the imposed fatigue cycles below 50% of characteristic lifetime, as shown in Fig. 5.27 and Table 5.11. However, at fatigue cycles between 50 and 75% of the characteristic lifetime, the loss in tenacity and elongation at break is almost twice the amount suffered up to 50% of characteristic lifetime; beyond fatigue cycles equal to 75% of the characteristic lifetime there is a precipitous and profound loss in tenacity and elongation at break. The survivors, after experiencing fatigue cycles equivalent to their characteristic lifetimes, i.e., 100% level, have a residual tenacity and elongation at break equal to only 30 and 55%, respectively, of their respective values before being subjected to any fatigue. Such sudden losses in tenacity and elongation at break beyond fatigue cycles equal to 75% of characteristic lifetime perhaps indicate the possibility of potential failure of yarns on the loom if the yarns experience a fatigue level of similar magnitude and the actual tension imposed during weaving exceeds the residual tenacity. The progressively increasing deterioration of the tensile properties with the increasing fatigue level may explain why the same yarns sized at a particular add-on and from the same ingredients under identical slashing conditions behave differently on different types of looms. The yarns which work satisfactorily on automatic shuttle looms may perhaps fail to work satisfactorily on high-speed shuttleless weaving machines.

Visual Damage Criterion. This criterion of evaluating fatigue damage, though subjective in nature, yields useful information regarding microstructural damage of yarns which occurs during the coarse of fatiguing. The survivors of yarns obtained after subjecting to known intensity and level of fatigue

Table 5.11 Rate of Fatigue Damage Expressed in Terms of Loss in Tenacity and Elongation at Break

Percentage of characteristic lifetime	Tenacity (cN/tex)	Elongation at break (%)	Loss in tenacity (%)	Loss in elongation (%)
0	18.66	8.32	—	—
25	17.14	7.90	8.14	5.05
50	16.11	7.62	13.66	8.41
75	13.42	7.12	28.11	14.42
100	5.55	4.61	70.26	44.59

Source: Ref. 37.

accompanied by abrasion action were collected and mounted on a stub for scanning electron microscope studies. A typical SEM photograph of a portion of sized ring spun yarn subjected to abrasion and fatigue (450 cycles/min, 0.5% strain amplitude, 3 cN/tex pretension and 2.5 mm abrasion pin position) is shown in Fig. 5.28. The photograph shows a complete and partial rupture of some of the fibers caused by intensive abrasion action. The severity of the damage inflicted on the fibers under cumulative tensile fatigue, however, was influenced by the intensity and level of fatigue and abrasive actions and the properties of fibers, such as tensile, frictional, bending, and the nature of spin finish in the case of synthetic fibers. This type of visual study may be used in understanding the relative differences in fatigue behavior of similar yarns spun on different spinning systems.

Effect of Webtester-Related Parameters on Fatigue Behavior

Anandjiwala and Goswami [37] reported experimental work on 20 tex sized ring and open-end spun yarns using the webtester and the following parameters: 450 cycles/min, 2.5 mm abrasion pin deflection, 3 cN/tex base tension, and 0.5% strain amplitude. To isolate the effect of each parameter, the parameter under investigation was systematically varied by keeping all other parameters constant. Since this study was not intended for comparison of fatigue resistance of ring and open-end spun yarns, the separate results were given

Fig. 5.28 SEM photomicrograph representing visual fatigue damage. (From Ref. 37.)

for the different yarn types. The trends and results obtained were, however, consistent for both yarn types.

Effect of Base Tension. The results of the effect of base tension on the fatigue behavior of ring-spun yarns from the above-mentioned study [37] are shown in Fig. 5.29. The characteristic lifetime linearly decreased with an increase in the base tension at which the yarns were mounted on the webtester as expected. There is an almost five times reduction in characteristic lifetimes when the base tension is increased from 2 to 5 cN/tex. The straight line fitted by regression analysis is shown by the solid line in Fig. 5.29. The slope and intercept of this fitted straight line are -818.38 and 4387, respectively, with a correlation coefficient (r) equal to -0.98. However, no clear trend was noticed between base tension and the scalar parameter determining the shape of the Weibull distribution. This is due to the fact that consideration of only characteristic lifetime does not give the entire picture of the distribution of lifetime that normally occurs. Therefore, it is always much more informative to observe the effect in terms of complete distributions at all base tension levels. Figure 5.30 shows the fitted Weibull distribution for the yarn tested at

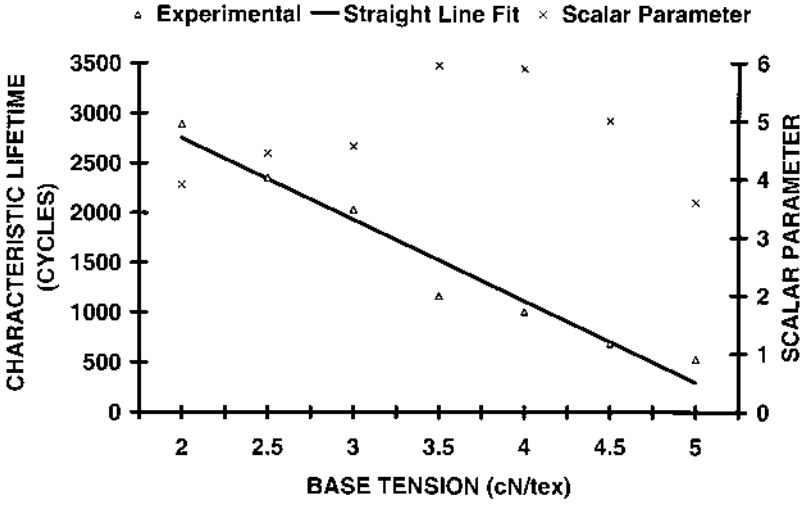

Fig. 5.29 Effect of base tension on fatigue behavior of open-end spun yarn. (△) Characteristic lifetime; (——) fitted straight line; (×) scalar parameter. (From Ref. 37.)

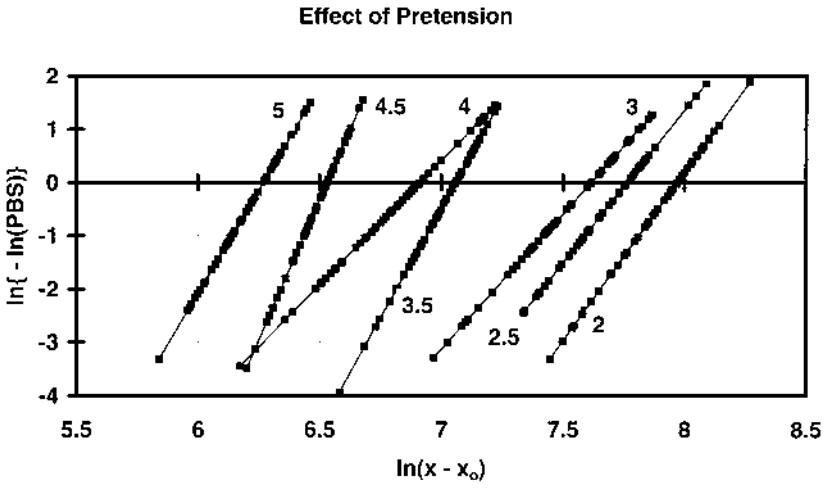

Fig. 5.30 Weibull distribution fit showing the effect of base tension at 2.0, 2.5, 3.0, 3.5, 4.0, 4.5, and 5.0 cN/tex for open-end yarn. (From Ref. 37.)

all base tension levels shown in Fig. 5.29. From Fig. 5.30 it is apparent that the entire distribution for any particular base tension level shifts toward the left, which indicates a reduction in fatigue resistance. This is consistent with what is shown in Fig. 5.29.

Scanning electron micrographs of two ruptured ends of a yarn fatigued at the same number of cycles but at various base tensions are shown in Plates 5.1–5.4. The plates denoted by A and B are photomicrographs of the same yarn at lower (27×) and higher (100×) magnifications, respectively. It is obvious from Plates 5.1A–5.4A that the progressive deterioration of the yarn increases as the base tension is increased from 2 to 5 cN/tex. With the increase in base tension more fibers fray out at the ruptured yarn ends, perhaps because of higher intensity of abrasion. The photomicrographs taken at higher magnification reveal the partial and complete rupture, peeling-off, curling, and severe surface damage of some of the fibers, particularly at higher base tension levels. The failure of the yarn is caused by the mixed mode of fatigue and abrasion actions. The isolation of the effect of simple fatigue and simple abrasion on the rupture of the yarns was not considered by the authors [37] because their formative research work was primarily intended for understanding the yarn fatigue and its effect on the performance of yarns during weaving. Yarns are

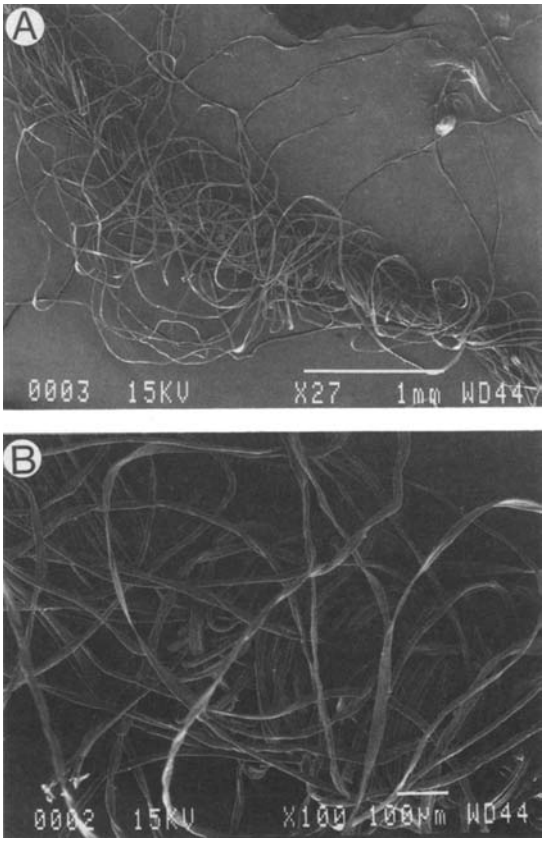

Plate 5.1 SEM photomicrograph of open-end spun yarn fatigued at a speed of 450 cycles/min, base tension of 2 cN/tex. strain amplitude of 0.5% and abrasion pin deflection of 3.0 mm, magnification (A) 27× and (B) 100×. (From Ref. 37.)

always subjected to combined actions of abrasion and cyclic extension fatigue on a loom, and the webtester simulates all the major forces that occur [32,33].

Trauter et al. [39] found similar results in their experiments on the effect of pretension on the abrasion resistance of 20 tex cotton yarn, fatigued at a strain amplitude of 0.5% and abrasion pin position of 3.0 mm, as shown in Fig. 5.31. They estimated the abrasion resistance for first and sixth breaks, denoted as ST(1) and ST(6), respectively, at base tensions of 5, 10, 20, and

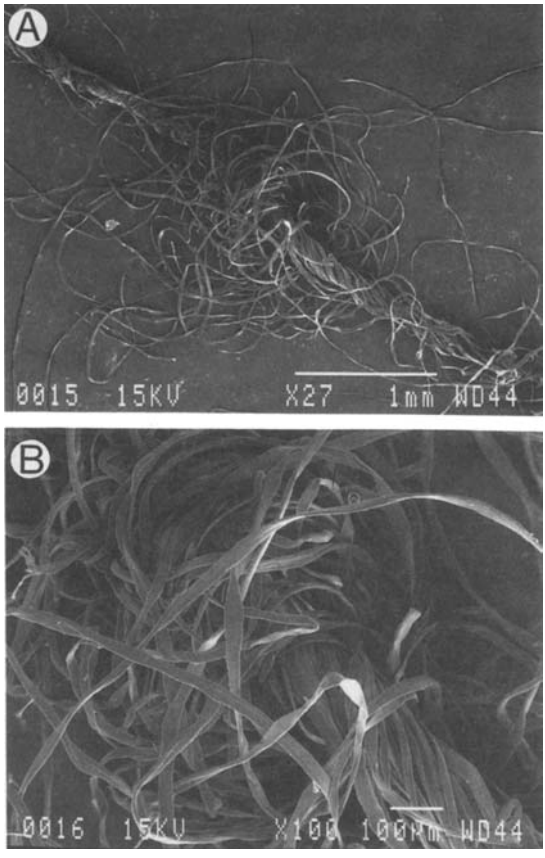

Plate 5.2 SEM photomicrograph of open-end spun yarn fatigued at a speed of 450 cycles/min, base tension of 3 cN/tex. strain amplitude of 0.5% and abrasion pin deflection of 3.0 mm, magnification (A) 27× and (B) 100×. (From Ref. 37.)

30 cN (0.25, 0.5, 1.0, and 1.5 cN/tex), as shown in Fig. 5.31. In general, the abrasion resistance decreased with an increase in base tension, as shown in Fig. 5.31.

An increase in the base tension at which the yarn specimens are mounted on the webtester at a constant deflection of abrasion pin results in an increase in the transverse pressure between the yarn and the abrasion pin, which in turn results in an increase in intensity of abrasion. A high intensity of abrasive

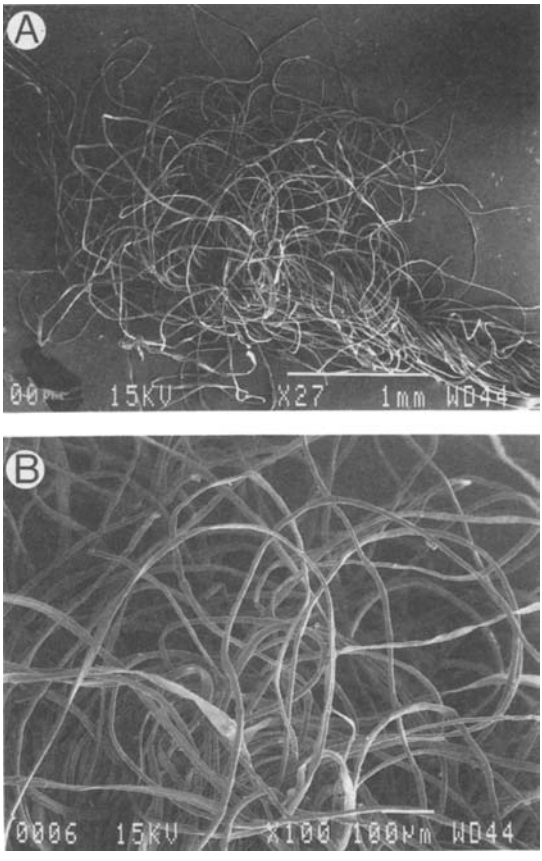

Plate 5.3 SEM photomicrograph of open-end spun yarn fatigued at a speed of 450 cycles/min, base tension of 4 cN/tex. strain amplitude of 0.5% and abrasion pin deflection of 3.0 mm, magnification (A) 27× and (B) 100×. (From Ref. 37.)

action, which is associated with higher tension, obviously will cause an accelerated deterioration of the yarn properties. It may be argued that the higher base tension may tend to increase the consolidation of the fibers in a yarn, which should result in a better tensile resistance; however, the increased severity of the abrasion action perhaps overshadows the consolidation effect. The net effect of these two opposing actions appears to result in decreased fatigue resistance.

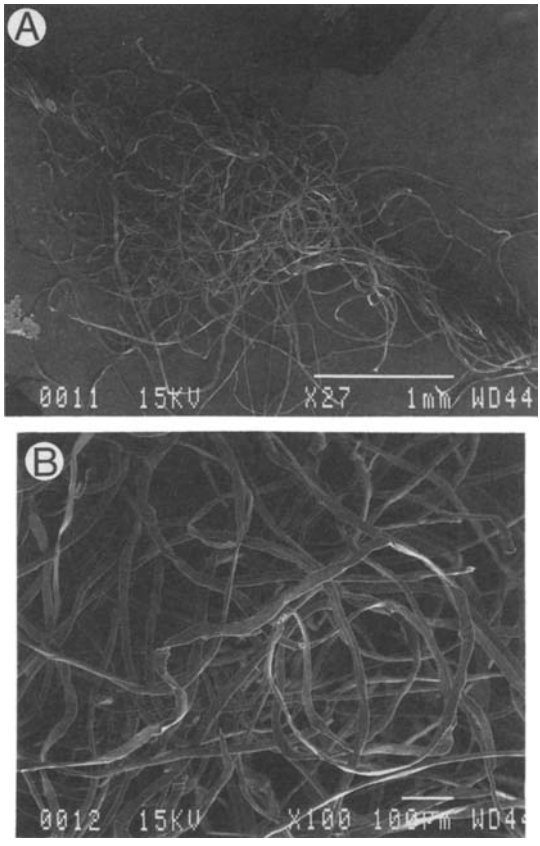

Plate 5.4 SEM photomicrograph of open-end spun yarn fatigued at a speed of 450 cycles/min, base tension of 5 cN/tex. strain amplitude of 0.5% and abrasion pin deflection of 3.0 mm, magnification (A) 27× and (B) 100×. (From Ref. 37.)

Effect of Abrasion Pin Position. The results of the same study [37] reported the effect of abrasion pin position on the characteristic lifetime and scalar parameter of the Weibull distribution for ring-spun yarns, and the results are shown in Fig. 5.32. With an increase in abrasion pin position from 1.5 to 2.0 mm the fall in fatigue resistance of the yarns is very pronounced, as is obvious from Fig. 5.32. Beyond a 2.0-mm abrasion pin deflection, the fatigue resistance of the yarn progressively decreases until it reaches a value of 516

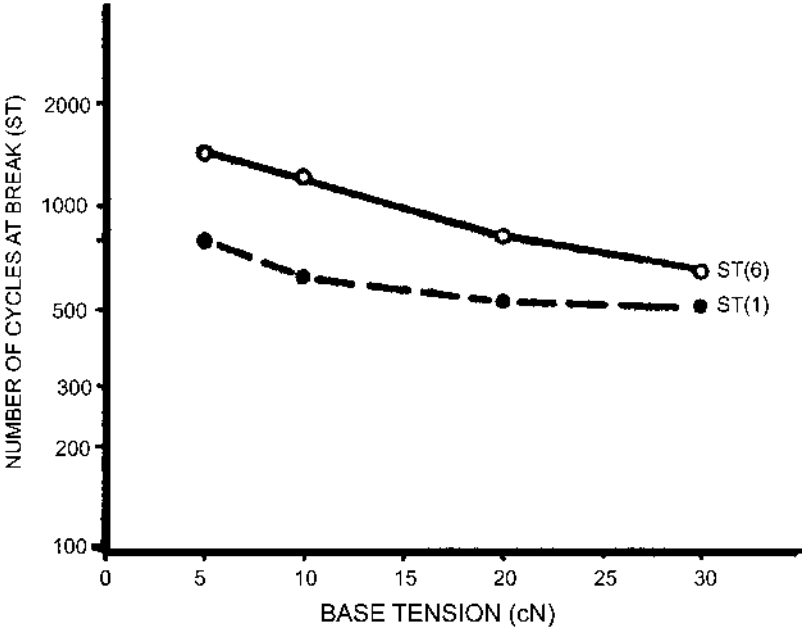

Fig. 5.31 Effect of base tension on abrasion resistance characteristics. (From Ref. 39.)

cycles at 5.0 mm. The increase in abrasion pin deflection on the webtester geometrically increases the contact angle of the test yarn around the circular pin, as shown in Fig. 5.33. This results in increased frictional forces between the yarn and the abrasion pin. The increase in yarn tension is a consequence of an increase in the deflection of the abrasion pin. The combined effect of these two actions tends to decrease the fatigue resistance of the yarn. The trend of changes in scalar parameter with respect to increased deflection pin position is not clear from Fig. 5.32. Figure 5.34 shows the fitted Weibull distribution for the yarns tested at different abrasion pin positions. Though the slope of individual lines varies slightly, the trend of the entire distribution shifting toward the left—meaning decreasing fatigue resistance—is clearly noticeable.

Trauter et al. [39] also studied the effect of abrasion intensity on the abrasion resistance of 20 tex cotton yarn, tested at a strain amplitude of 0.5% and a base tension of 10 cN (0.5 cN/tex), as shown in Fig. 5.35. They estimated

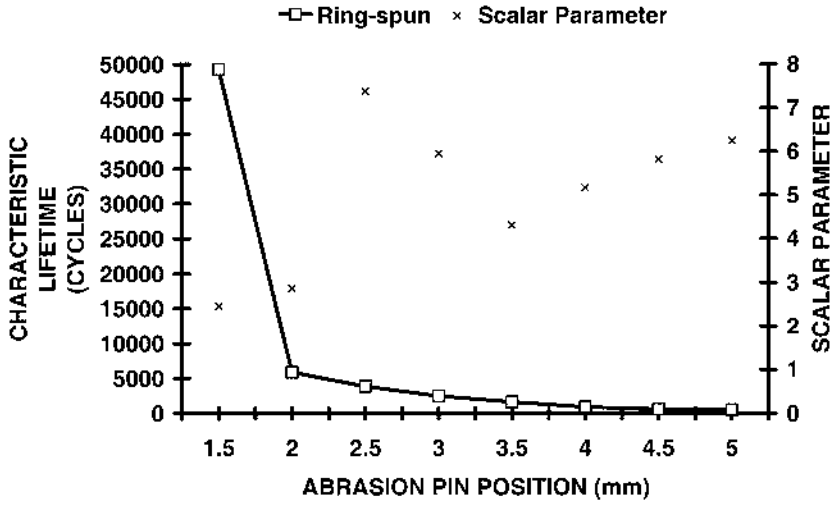

Fig. 5.32 Effect of abrasion pin position on fatigue behavior of ring-spun yarn. (□) Characteristic lifetime; (×) scalar parameter. (From Ref. 37.)

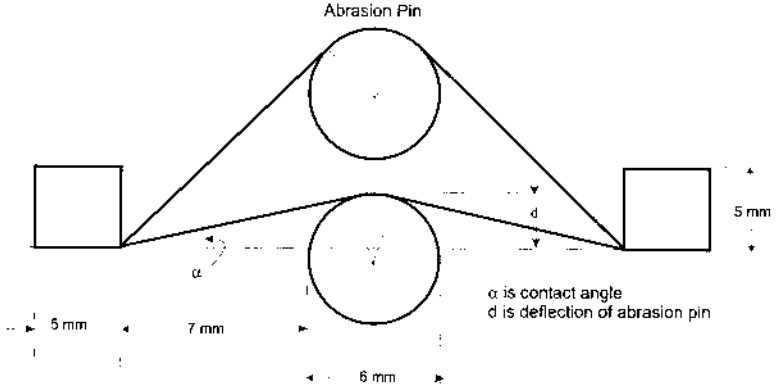

Fig. 5.33 Geometry of abrasion pin on the webtester. (From Ref. 37.)

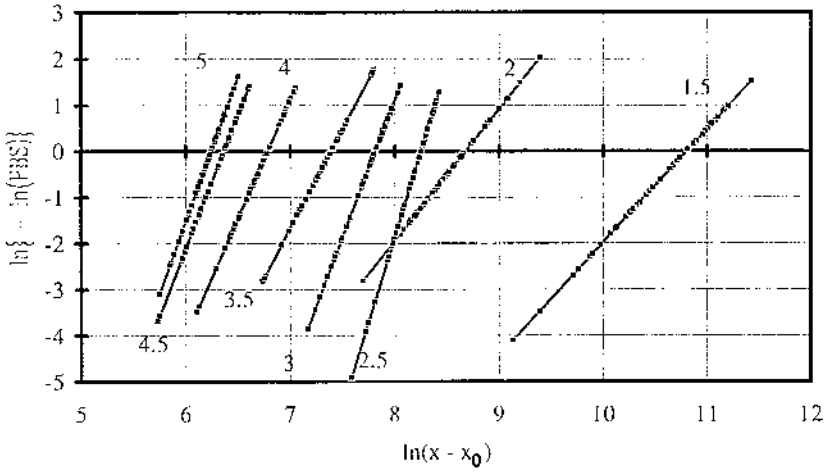

Fig. 5.34 Weibull distribution fit representing effect of abrasion pin deflection at 1.5, 2.0, 2.5, 3.0, 3.5, 4.0, 4.5, and 5.0 mm for ring-spun yarn. (From Ref. 37.)

the abrasion resistance for the first and sixth breaks, denoted as ST(1) and ST(6), respectively, at an abrasion pin penetration of 2.5, 3.0, 3.5, and 4.0 mm, as shown in Fig. 5.35. The abrasion resistance generally decreased with an increase in the abrasion pin penetration, as shown in Fig. 5.35.

Besides the deflection, the characteristics of the abrasion pin in terms of its surface roughness, material, size, and shape may also affect the fatigue resistance. Very rough surfaces will tend to reduce the fatigue resistance of the yarn, whereas very smooth surfaces such as glass may enhance the fatigue resistance because of the decreased abrasion resulting from the lower frictional coefficient. Similarly, abrasion pins with triangular or square cross sections may tend to increase the abrasive action due to sharp corners in comparison to polished round cross sections, resulting in rapid deterioration of the yarn. A polished brass pin having circular cross section with a 6-mm diameter was used but the effect of pin characteristics was not explored in this work [37].

Effect of Speed of Fatiguing. Figure 5.36 shows the effect of speed of fatiguing on the characteristic lifetime and scalar parameter of the Weibull distribution for the ring spun yarns [37]. With an increase in speed of fatiguing, in general, the characteristic lifetime decreases; however, the scatter observed is somewhat larger. The straight line fitted by the regression method is shown

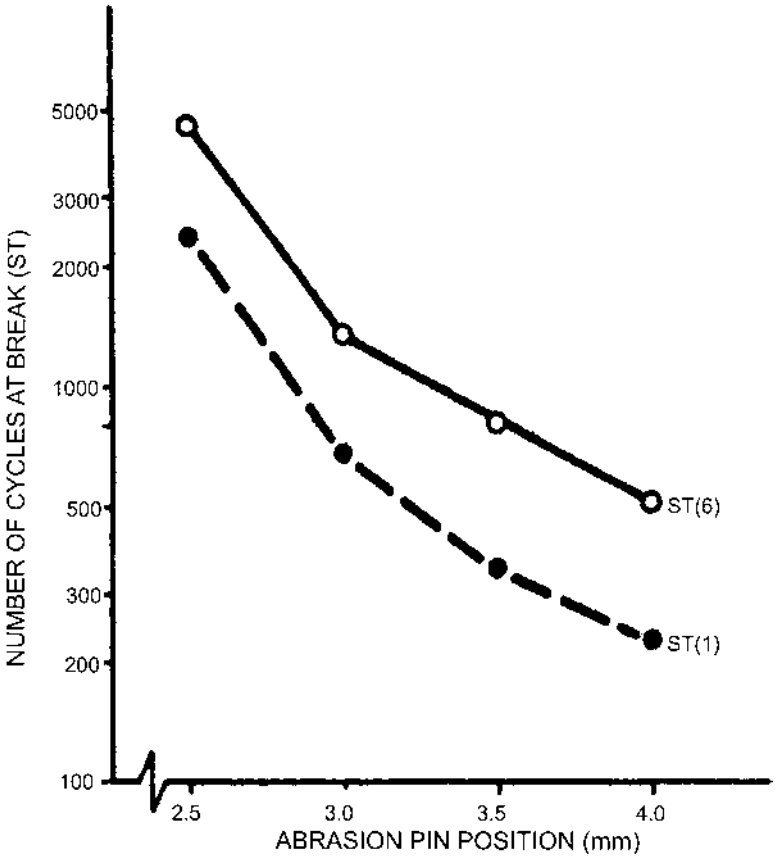

Fig. 5.35 Effect of abrasion pin position on abrasion resistance characteristics. (From Ref. 39.)

by a solid line in Fig. 5.36. The slope and intercept of this straight line are −1.94 and 3584.5, respectively, with a correlation coefficient (r) equal to −0.72, which is rather poor. The effect of increasing the fatigue speed on scalar parameter is not very clear, as seen in Fig. 5.36. Because of the wide scatter observed in the scalar parameter, and to some extent also in characteristic lifetime, the plotting of the entire Weibull distribution at each speed level has turned out to be somewhat difficult.

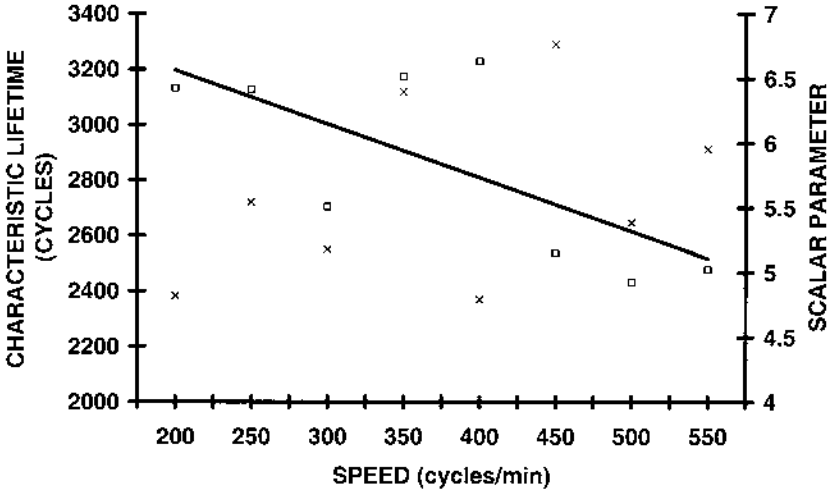

Fig. 5.36 Effect of speed of fatiguing on fatigue behavior of ring-spun yarn. (□) Characteristic lifetime; (——) fitted straight line; (×) scalar parameter. (From Ref. 37.)

Scanning electron photomicrographs of two ends of a ruptured yarn are shown in Plates 5.5, 5.2, and 5.6 tested at 350, 450, and 550 cycles/min respectively. The plates denoted by A and B are the photomicrographs of the same yarn at lower (27×) and higher (100×) magnifications, respectively. At a low speed of fatiguing (350 cycles/min) the fibers were partially pulled away from the yarn matrix with one end still remaining in the yarn. The fibers are partially displaced from the surface of the yarn and coiled around adjacent fibers. The yarn rupture is principally a result of the abrasive action of the pin. At higher speeds of fatiguing, the resultant damage to the yarn is more severe because of the rapidity of the combined actions of abrasion and extension fatigue. The photographs taken at higher magnification show partial and complete breakage, peeling-off, surface damage due to abrasion, and curling-off of some fibers.

Effect of Strain Amplitude. Figure 5.37 shows the effect of change in strain amplitude on the characteristic lifetime and scalar parameter of the Weibull distribution for ring spun yarns, as reported in the same study [37]. The increase in strain amplitude, in general, tends to decrease the characteristic lifetime of the yarns. At constant speed of fatiguing, the strain amplitude

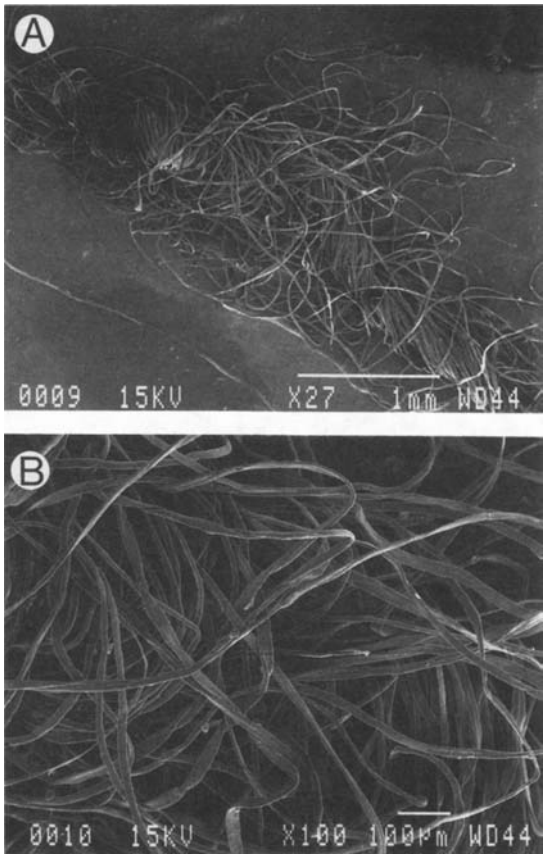

Plate 5.5 SEM photomicrograph of open-end spun yarn fatigued at a speed of 350 cycles/min, base tension of 3 cN/tex. strain amplitude of 0.5% and abrasion pin deflection of 3.0 mm, magnification (A) 27× and (B) 100×. (From Ref. 37.)

determines the amount by which the yarn is extended on every cycle: the higher the strain amplitude, the greater is the cyclic extension, resulting in a higher intensity of fatigue action. The regression line is shown by the solid line in Fig. 5.37. The slope and the intercept of this fitted straight line are −2001.3 and 2836, respectively, with a correlation coefficient (r) equal to −0.93. However, there appeared to be no noticeable relationship between

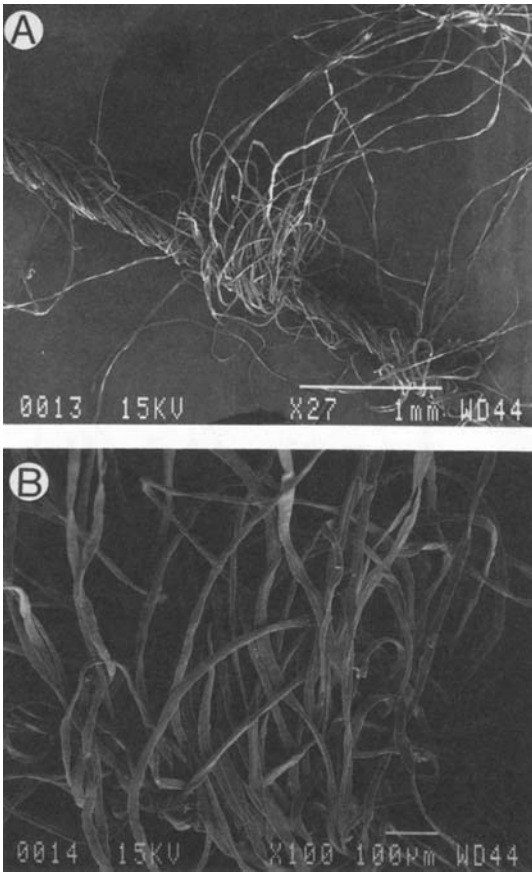

Plate 5.6 SEM photomicrograph of open-end spun yarn fatigued at a speed of 550 cycles/min, base tension of 3 cN/tex. strain amplitude of 0.5% and abrasion pin deflection of 3.0 mm, magnification (A) 27× and (B) 100×. (From Ref. 37.)

scalar parameter and strain amplitude. Figure 5.38 shows the composite plot of the fitted Weibull distribution for all strain amplitude levels.

Trauter et al. [39] also studied the effect of strain amplitude on the abrasion resistance of 14.3 and 20 tex cotton yarns fatigued at a pretension of 10 cN and pin penetration of 3 mm, as shown in Fig. 5.39. They again estimated the abrasion resistance for the first and sixth breaks, denoted as

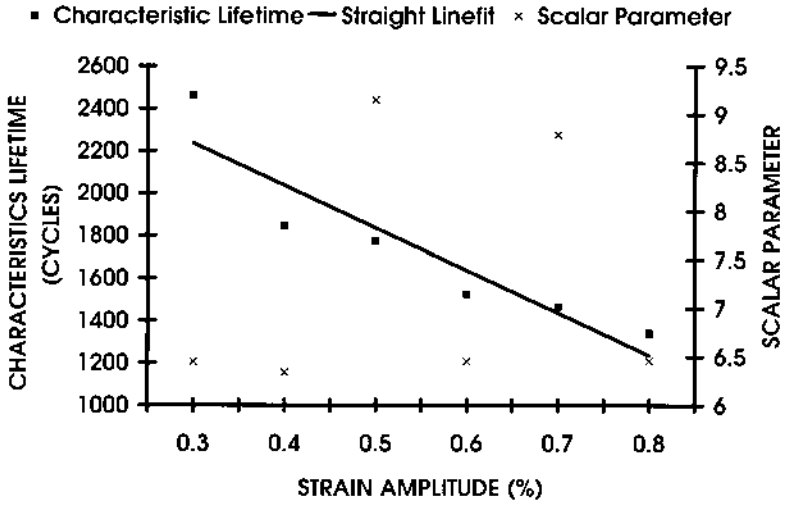

Fig. 5.37 Effect of strain amplitude on fatigue behavior of ring-spun yarn. (□) Characteristic lifetime; (——) fitted straight line; (×) scalar parameter. (From Ref. 37.)

ST(1) and ST(6), respectively, at strain amplitudes of 0.3, 0.5, 0.8, and 1.1%, as shown in Fig. 5.39. The abrasion resistance generally decreased with an increase in strain amplitude, as shown in the figure.

The reduction in fatigue resistance of the yarn with increasing strain amplitude is attributed to the development of permanent ''set'' in the yarn when subjected to a cyclical elongation of higher magnitude. The cyclical extension of the yarn beyond its yield point results in a residual elongation, which gradually increases under cumulative fatiguing process; consequently, the yarn either exhibits actual rupture because it weakens or it develops slack which may be classified as a pseudobreak.

Practical Applications

The realistic practical applications of fatigue/abrasion behavior of sized yarns as evaluated on the Sulzer-Ruti Webtester in the laboratory may be directed to assess the efficiency of various size formulations applied at various add-on levels, the efficiency of different size types and their mixtures, the performance behavior of various yarn types, and the optimization of processing variables on a slasher, even without conducting costly and time-consuming in-plant

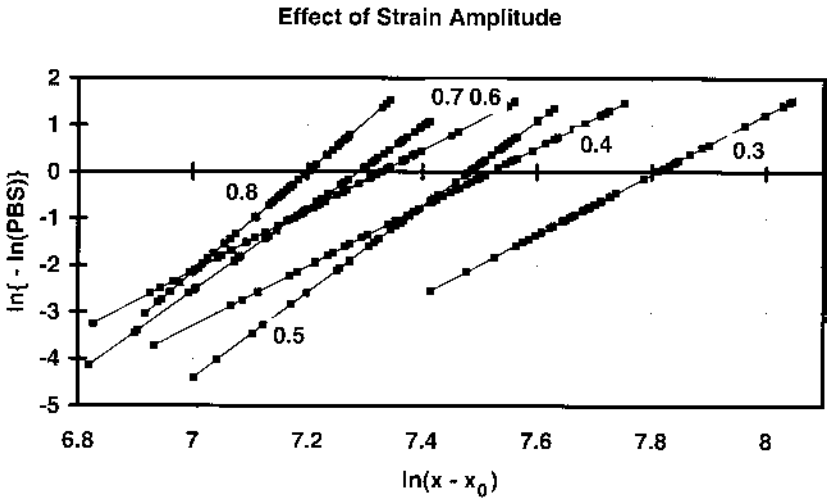

Fig. 5.38 Weibull distribution fit representing effect of strain amplitude at 0.3, 0.4, 0.5, 0.6, 0.7, and 0.8% for ring-spun yarn. (From Ref. 37.)

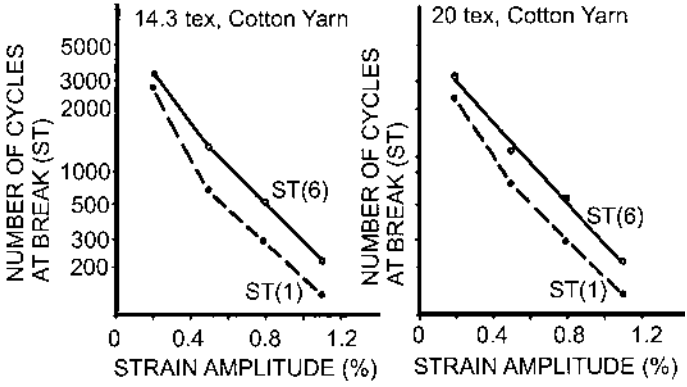

Fig. 5.39 Effect of strain amplitude on abrasion resistance characteristics. (From Ref. 39.)

weaving trials. However, the confidence level of using the technique to assess fatigue/abrasion failure of sized yarns developed by Anandjiwala and Goswami [37] and several other authors [39–42,57,58,63–68] depends upon the positive correlation between the laboratory evaluation on the webtester and the actual weaving trials on the loom. Indeed, the task is enormous, because for setting up such correlation a large amount of experimental work is required to be conducted on different types of yarns, different size types, different size formulations, and on different types of looms. The research work leading to establish basic principles and a methodology to link the laboratory evaluation of fatigue/abrasion behavior as measured on the webtester to that on a loom is a step in the right direction. The following is a discussion of the methodology established and the analysis technique developed to assess the laboratory evaluation of fatigue based on failure criteria that can be advantageously used in practical situations.

Figure 5.40 shows the effect of size mixtures on a 20 tex, 50/50 cotton/polyester open-end yarn sized at 9% nominal size add-on level. The entire Weibull distribution fitted to the experimental results of fatigue measured on the webtester [39,40] for the same yarn sized with Recipe C (70% PVA + 22% starch + 8% wax) and Recipe A (50% PVA + 42% starch + 8% wax) is plotted using the technique developed by the authors [37]. The rightward shift of the entire distribution indicates improvement in the fatigue resistance of the yarns. The fatigue resistance of the unsized yarns, as expected, is poor. The effect of size application manifests itself in the improvement in fatigue resistance due to the cementing action of the fibers in the yarn and enhancement in abrasion resistance. Figure 5.40 shows the usefulness of the laboratory technique employed in showing that the yarn sized with Recipe C performs distinctly better than that sized with Recipe A. Such initial laboratory trials help in assessing various size mixtures without conducting the time-intensive and costly in-plant trials.

Figure 5.41 shows the relative fatigue performance of 20 tex, 50/50 cotton/polyester ring and open-end spun yarns sized at 9% nominal size add-on with the size mixture containing 70% PVA + 22% starch + 8% wax. The distinct rightward shift of the entire distribution of the fatigue behavior of the open-end spun yarn indicates comparatively better resistance than that of the ring-spun yarn. This is attributed to the relative differences in the structure of the yarns spun on different spinning systems. Perhaps, the open-end yarn with a relatively open yarn structure facilitates better penetration and migration of size mixture resulting in a better cementing action of fibers in the yarn core. The ring-spun yarn with a compact twist geometry does not allow substantial size penetration and migration. Perhaps more size is deposited

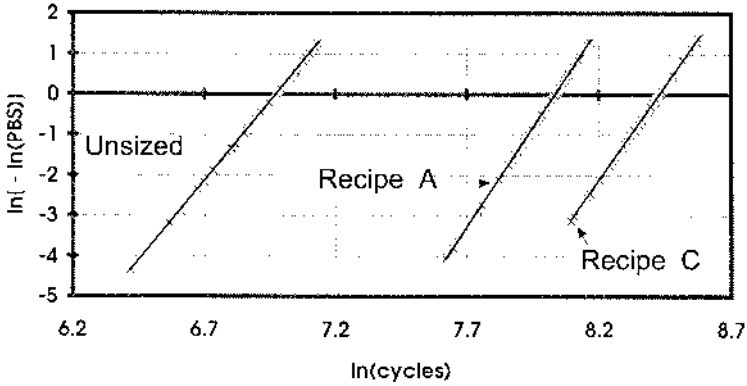

Fig. 5.40 Effect of size mixtures on fatigue behavior of 20 tex, 50/50 cotton/polyester open-end yarn, Recipe A: 50% PVA + 42% starch + 8% wax; Recipe C: 70% PVA + 22% starch + 8% wax. (From Ref. 37.)

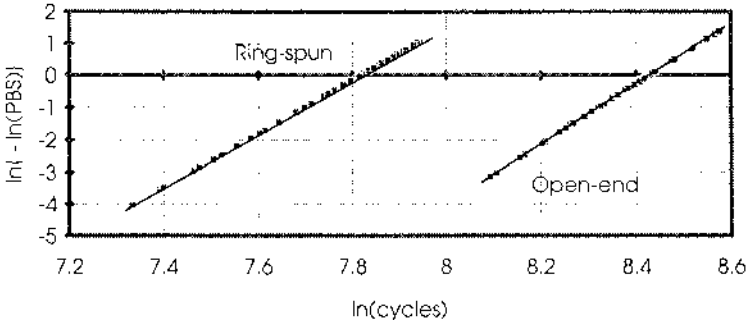

Fig. 5.41 Relative fatigue performance of 20 tex, 50/50 cotton/polyester ring- and open-end spun yarns sized at 9% add-on level of 70% PVA + 22% starch + 8% wax mixture. (From Ref. 37.)

on the surface of the ring-spun yarn, resulting in easy size shed-off due to the applied abrasion during testing on the webtester. This interesting feature of the same size mixtures applied to different yarn types under identical processing and testing conditions can be easily estimated using the laboratory technique. Such laboratory studies help in optimizing size mixture, add-on level, and processing conditions for yarns spun on different spinning systems.

Trauter et al. [39] used the webtester to study the effect of size add-on (degree of sizing) on the abrasion resistance of yarns. They prepared a ''life characteristics curve'' of the yarn at different size add-on levels, as shown on the left-hand side of Fig. 5.42. Then they plotted the abrasion characteristics ST(1) and ST(6) of the life characteristics curve against the degree of sizing on a semi-logarithmic scale, as shown on the right-hand side of Fig. 5.42, to characterize the abrasion resistance. The abrasion resistance increases with an increase in size add-on. The abrasion characteristics of the yarns ''sized'' with water only also lie on this graph, shown by the arrow at 0% size add-on, which represents the lower limit of the abrasion resistance of the warp yarns.

A sizing recipe that requires less size add-on to achieve the same abrasion characteristics can be regarded as more effective. Trauter et al. [39] studied the efficiency of two different size recipes by means of abrasion characteristics,

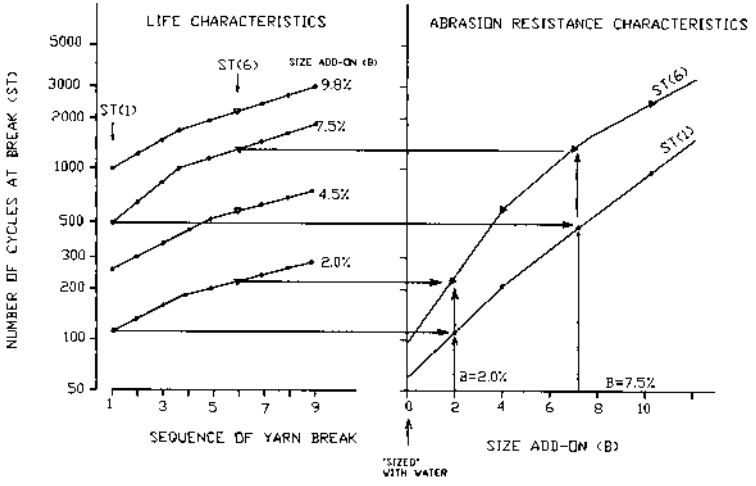

Fig. 5.42 Effect of size add-on on life characteristics and abrasion resistance of yarn. (From Ref. 39.)

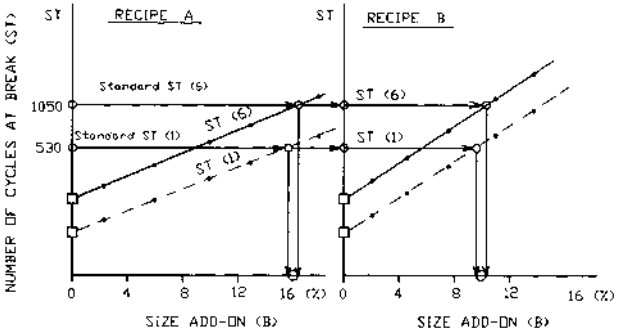

Fig. 5.43 Effectiveness of size recipes measured in terms of abrasion resistance characteristics. (From Ref. 39.)

denoted by ST(1) and ST(6) in their analysis of tests conducted on the webtester. They sized the same yarn with two different size recipes, denoted by Recipe A and Recipe B, at different levels of add-on on a pilot sizing plant at Reutlingen. The abrasion characteristics were measured and plots were prepared for both sizing recipes, as shown in Fig. 5.43. To develop standards for comparison purposes, the authors measured the abrasion characteristics, ST(1)* and ST(6)*, on the webtester of the same yarns with the same size recipes but sized on industrial sizing machines. As shown in Fig. 5.43, at the same level of abrasion characteristics (e.g., ST(1)* = 530 cycles and ST(6)* = 1050 cycles) of the industrially sized warp yarns, the size add-on required for Recipe A is almost 16.3%, whereas for Recipe B only 9.8% is required. This implies that Recipe B is more effective than Recipe A as a lower size add-on is required to achieve the same abrasion resistance. Trauter et al. [39] also made a comparison for a 16.7 tex, 65/35 polyester/cotton blended yarn, sized with different sizing agents using similar methodology. Table 5.12 shows the minimum size add-on required to achieve the standard abrasion characteristics of ST(1)* = 380 and ST(6)* = 850.

Trauter et al. [39,72,73] also attempted to develop a correlation between the abrasion characteristic ST(6) and the warp yarn breakages on the loom. The warp samples (30 tex, 100% cotton and 30 tex 67/33 polyester/cotton) sized in the mills under normal conditions were tested for abrasion characteristics ST(6) on the webtester and correlated with the actual warp breaks during weaving, as shown in Fig. 5.44. The authors claimed that it was possible to predict the actual performance of warp yarns during weaving by testing sam-

Table 5.12 Necessary Size Add-On to Achieve Standard Abrasion Characteristics

Tested sizing agent	Necessary size add-on (%)	Equivalent quantities
Starch	18.2	1
PVA	6.0	0.33
Polyacrylate	7.9	0.43

Note: For ST(1)* = 380 and ST(6)* = 850 cycles.
Source: Ref. 39.

ples on the webtester for assessing the life characteristic curve and abrasion characteristics ST(6). The results reported by Trauter et al. [39] were limited to only a few trials; however, they reported a confidence level of more than 80% based on their experience.

The methodology introduced in this section provides information about the usefulness of the webtester for assessing the weaving performance of sized warp yarns in the laboratory. The mills can attempt a variety of sizing- and yarn-related measurements by using the webtester and prepare their own data which can be used with considerable confidence.

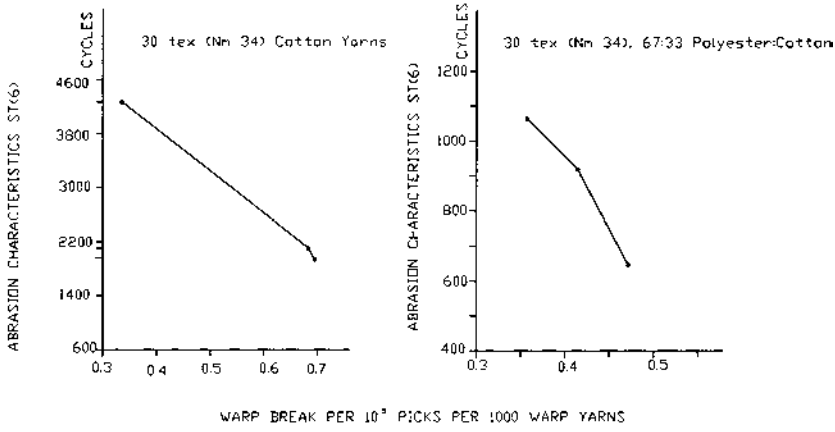

Fig. 5.44 Correlation between abrasion characteristics and warp break during weaving. (From Ref. 39.)

REFERENCES

1. Bradbury, E. The testing of sizes for continuous filament yarns of high filament strength. J. Text. Inst. 1949, 40, T299–T310.
2. Bradbury, E.; Hacking, H. experimental technique for mill investigation of sizing and weaving. J. Text. Inst. 1949, 40, T532–T553.
3. Bradbury, E. The Effect of sizing on warp breakage. J. Text. Inst. 1949, 40, P272–P276.
4. Ranganathan, S.R.; Verma, B.C. Laboratory evaluation of the performance of sized yarn. Textile Recorder. 1967, LXXXV(No. 1017), 34–35.
5. Jackle, R.W.; Burnett, R. TRS technique for size evaluation. Am. Dyestuff Reporter. 1967, 56, 11–13.
6. Trost, H.B.; Bush, H.B. Sizing up warp sizes. Textile Industries. 1970, 134(No. 6), 127–134.
7. Trauter, J.; Laupichler, M. Data sheets for sizing agents, from the Institut fur Textiltechnik Reutlingen (ITR). Melliand Textilberichte. 1976, 57(No.5), 375–379; No. 6, 443–444; No. 7, 545–548; No. 8, 625–626; No. 9, 713–714; No. 10, 797–798; No. 11, 875–876: No. 12, 979–980.
8. Blumenstein, C.R. Size and fiber/yarn relationship, part 1. Textile Industries. 1969, 133, 93, 95–97.
9. Grimshaw, A.H. The tensile strength of sized and unsized cotton warps. Melliand. 1930, 2, 1050, 1178.
10. Faasen, N.J.; van Harten, K. The effect of sizing on the weavability of cotton yarns. J. Text. Inst. 1966, 57, T269–T285.
11. Faasen, N.J.; van Harten, K. The effect of sizing on the weavability of cotton yarns (Reply to Letter to the Editor). J. Text. Inst. 1967, 58, pp 87–88.
12. Furry, M.S. Stiffness produced in fabrics by various starches and sizing mixtures. J. Home Econ. 1933, 25, 143.
13. Furry, M.S. Strength produced in different fabrics by various starches and modified starches. J. Home Econ. 1936, 28, 687.
14. Preston, E.C.; Dantzig, T. Stiffness in fabrics produced by different starches and starch mixtures and a quantitative method for evaluating stiffness. U.S. Department of Agriculture Tech. Bull. 1929(No. 108), 30.
15. Frankenberg, G.; Sookne, A.M.; Harris, M. Weaving efficiency and film properties of warp sizing materials, in Spun Rayon Warp Sizing, Textile Research Institute. 1945, 65–90.
16. Neale, S.M. The elasticity and tensile strength of starch. J. Text. Inst. 1924, 15, T443–T452.
17. Peirce, F.T. The influence of humidity on the elastic properties of starch film. J. Text. Inst. 1928, 19, T237–T252.
18. Swan, E. Absorption of water by dried films of boiled starch: absorption and desorption between 20°C and 90°C. J. Text. Inst. 1926, 17, T527–T536.
19. King, D.E.; Weil, H.A.; Condo, F.E.; Rutherford, H.A. The evaluation of textile sizes. Text. Res. J. 1952, 22, 567–573.

20. Schutz, R.A. Theoretical and practical aspects of sizing, in Technology of Warp Sizing. Smith J.B., Ed.; Columbine Press: London, 1964, 65–92.
21. Schutz, R.A. Theoretical and practical aspects of sizing today and tomorrow, Third International Sizing Symposium; Shirley Institute: Manchester, England, 1977, 1–11.
22. Owen, A. E.; Oxley, A.E. The physical properties of yarns under oscillating stresses. J. Text. Inst. 1923, 14, T18–T27.
23. Owen, A.E. The physical properties of yarns under oscillating stresses, some physical tests on sized yarns. J. Text. Inst. 1923, 14, T375–T389.
24. Matthew, J.A. Effect of sizes on the elastic behavior of flax yarns. J. Text. Inst. 1926, 17, T192.
25. Schreiber, W.T.; Geib, M.N.V.; Moore, O.C. Effect of sizing, weaving and abrasion on the physical properties of cotton yarn (RP993). J. Res. Natl. Bur. Standards. 1937, 18, 559.
26. Owen, A.E.; Locke, J. The measurement of resistance of yarns to abrasion. J. Text. Inst. 1926, 17, T567–T582.
27. Ramirez, R.P.; Vidosic, J.P. The loom-action-type abrader (Letter to the Editor). Text. Res. J. 1956, 26, 532–533.
28. Mehta, P.C.; Shah, C.C. Loom-action-type abrader (Letter to the Editor). Text. Res. J. 1957, 27, 169–170.
29. Radhakrishnan, T.; Mehta, P.C.; Shelat, B.R. The resistance of sized yarns to abrasion. Text. Res. J. 1957, 27, 439–444.
30. Trauter, J.; Schneider, H.J.; Laupichler, M. Sizing of dense warps. Melliand Textilberichte International. 1975, 56(No. 1), 16–20; No. 2, 114–117.
31. Trauter, J. The most important physical influences in the sizing process in relation to their effect on the weavability performance of the yarns. Textil Praxis International. 1973, 27(No. 4), 221–223; No. 5, 273–275; No. 8, 480–485; No. 10, 593–595 (1972) and 28, No. 1, 22–26.
32. Zolotarevskii, L.T. Effect of mechanical action in weaving on the technological properties of the warp yarn. Technol. Text. Ind. USSR. 1963(No. 6), 99–105.
33. Borodovskii, M.S.; Voronina, A. Yarn fatigue in cyclic extension. Tekstil. Prom. 1948, 10.
34. Milovidov, N.N. The cyclic tensile strength of yarn and its connection with the end-breakage rate in weaving. Technol. Text. Ind. USSR. 1964(No. 2), 75–79.
35. Davydov, A.F.; Kiryukhin, S.M.; Kukin, G.N. The statistical aspect of the variation of the strength of cotton yarn in cyclic extension. Technol. Text. Ind. USSR. 1970(No. 6), 12–14.
36. Forester, P.G. Fatigue of Metals; Pergamon Press: New York, 1962.
37. Anandjiwala, R.D.; Goswami, B.C. Studies of tensile fatigue behavior of staple yarns. Text. Res. J. 1993, 63, 392–403.
38. Lord, P.R.; Mohamed, M.H. Weaving: Conversion of Yarn to Fabric. Second Edition, Merrow: Durham, England; 1982.

39. Trauter, J.; Ruess, B.; Laupichler, M. Methods and tests to determine the weavability of sized yarn, Third International Sizing Symposium; Shirley Institute: Manchester, 1977, 67–92.
40. Trauter, J.; Weisenberger, W. Reutlinger Webtester. Textil Praxis International. 1979, 34, 1134–1135.
41. Trauter, J. Evaluation of processing behavior of sized yarns, Lecture to the Reutlingen Colloquim ''Processing Behavior of Fibers and Yarns'', of the Institute of Textile Technology, October 19–20, 1976; Meliand Textilberichte, 1977, 388–393.
42. Carmical III, W.N. Effect of tensile fatigue on warp yarn performance during high speed weaving Ph.D. Thesis; Clemson University: Clemson: SC, 1990.
43. ASTM Committee E-9 on Fatigue, Special Technical Publication, No. 91-A; Am. Soc. for Testing Materials: Philadelphia, 1958, 16.
44. Lyons, W.J. Fatigue in textile fibers. Part I: General considerations; fatiguing by cyclic tension: instrumentation and fatigue lifetimes. Text. Res. J. 1962, 32, 448–459.
45. Prevorsek, D.; Lyons, W.J.; Whitewell, J.C. Statistical treatment of data and extreme value theory in relation to fatigue in textiles. Text. Res. J. 1963, 33, 963–973.
46. Gumbel, E.J. Statistics of Extremes, Columbia University Press. 1958.
47. Weibull, W. Fatigue Testing and Analysis of Results; Pergamon Press: New York, 1961.
48. Hearle, W.S.; Sparrow, J.T. Tensile fatigue of cotton fibers. Text. Res. J. 1978, 48, 242–243.
49. Lyons, W.J.; Prevorsek, D.C. Law of cumulative damage in the fatigue of textile Fibers. Text. Res. J. 1965, 35, 1048–1049.
50. Prevorsek, D.C.; Lyons, W.J. Fatigue in textile fibers, Part V: Fatiguing by cyclic tension probability–strain–lifetimes relationships for a polyester sample. Text. Res. J. 1964, 34, 1040–1044.
51. Prevorsek, D.C.; Lyons, W.J. Fatigue in textile fibers. Part VI: Fatiguing by cyclic tension; effects of frequency on the statistics of lifetimes. Text. Res. J. 1965, 35, 73–78.
52. Prevorsek, D.C.; Lyons, W.J. Fatigue in textile fibers. Part IV: Fatiguing by cyclic tension; effects of stroke on the statistics of lifetimes. Text. Res. J. 1984, 34, 881–888.
53. Alihauskaite, G.; Piktis, A. Assessment of yarn fatigue from residual cyclic deformation. Technol. Text. Ind., U.S.S.R. 1966(No:2), 21–27.
54. Barella, A.; Bona, M. A tentative way to predict the performance of sized wool yarns in the loom. Inst. Inform. Text. 1967, 10, 233–246.
55. Borodovskii, N.S. Yarn ''fatigue'' and weaving productivity. Man-made Textiles. 1953, 32(380), 52–54.
56. Frank, F.; Singleton, R.W. A study of factors influencing the tensile fatigue behavior of yarns. Text. Res. J. 1964, 34, 11–19.

57. Picciotto, R.; Hersh, S.P. The tensile fatigue behavior of a warp yarn and its influence on weaving performance. Text. Res. J. 1972, 42, 512–522.
58. Picciotto, R.; Hersh, S.P. The fatigue behavior of a warp yarn and its influence on weaving performance—a response. Text. Res. J. 1973, 43, 430–431.
59. Budd, C.B. A fatigue test for tire cord. Text. Res. J. 1951, 21, 174–179.
60. Grant, J.N.; Couturier, G.M.; Rhodes, M.W. Effect of a dynamic fatigue test on the mechanical properties of tire cords. Text. Res. J. 1951, 21, 867–875.
61. Waller, R.C.; Roseveare, W.E. fatigue failure of rayon tire cord. J. Appl. Phy. 1946, 17, 482–491.
62. Busse, W.F.; Lessig, E.T.; Loughborough, D.L.; Larrick, L. Fatigue of fabrics. J. Appl. Phy. 1942, 13, 715–724.
63. Barella, A. On certain applications of Weibull's distribution to fatigue phenomena of yarns. Text. Res. J. 1965, 35, 1051–1053.
64. Barella, A. The application of the first and third asymptotic distributions to abrasion fatigue and repeated extension of yarns and to bending of fabrics. J. Text. Inst. 1965, 56, T665–T674.
65. Barella, A. The fatigue behavior of warp yarn and its influence on weaving performance. Text. Res. J. 1973, 43, 428–430.
66. Barella, A. The application of the first and third asymptotic distributions to abrasion fatigue and repeated extension of yarns and to bending of fabrics—a reply to the editor. J. Text. Inst. 1966, 57, T132–T134.
67. Sippel, A. The fatigue behavior of warp yarn and its influence on weaving performance. Text. Res. J. 1974, 725.
68. Stout, H.P. The application of the first and third asymptotic distributions to abrasion fatigue and repeated extension of yarns and to bending of fabrics—a letter to the editor. J. Text. Inst. 1966, 57, T131–T132.
69. Greene, W.H. Limdep User's Manual; 1986, 22.1–22.26.
70. Kalbfleisch, J.D.; Prentice, R.L. The Statistical Ananlysis of Failure Time Data; John Wiley and Sons: New York, 1980.
71. Gill, E.; Murray, W. Algorithms for the solution of the non-linear least squares problems. Siam. J. Numer. Anal. 1978, 15, 977–992.
72. Trauter, J.; Vialon, R. Estimating the weaving performance of sized staple fibre and filament yarns with the Reutlingen ''Webtester''. Textile Praxis International. 1985, 40, 1201–1204.
73. Trauter, J.; Gotz, K.; Vialon, R. Influence of yarn twist on the properties and weavability of sized warp yarns, Melliand Textilberichte. English Edition; 1/1989, E9–E11.